# Chapter 5

## Activation of the Nrf2 response by intrinsic hepatotoxic drugs correlates with suppression of NF-κB activation and sensitizes towards TNFα-induced cytotoxicity.

---

**This chapter has been published as:**

Bram Herpers¬*‡, Steven Wink*‡, Lisa Fredriksson*‡, Zi Di*, Giel Hendriks†, Harry Vrieling†, Hans de Bont* and Bob van de Water*§

‡ These authors contributed equally to the manuscript

*Division of Toxicology, Leiden Academic Centre for Drug Research, Leiden University, Leiden, The Netherlands

†Department of Human Genetics, Leiden University Medical Center, Leiden, The Netherlands

*Activation of the Nrf2 response by intrinsic hepatotoxic drugs correlates with suppression of NF-κB activation and sensitizes towards TNFα-induced cytotoxicity.*
Archives of Toxicology 2015 May 31. [Epub ahead of print]

1. **Abstract**

Drug-induced liver injury (DILI) is an important problem both in the clinic as well as in the development of new safer medicines. Two pivotal adaptation and survival responses to adverse drug reactions are oxidative stress and cytokine signalling based on activation of the transcription factors Nrf2 and NF-κB, respectively. Here we systematically investigated Nrf2 and NF-κB signalling upon DILI-related drug exposure. Transcriptomics analyses of 90 DILI compounds in primary human hepatocytes revealed that a strong Nrf2 activation is associated with a suppression of endogenous NF-κB activity. These responses were translated into quantitative high content live cell imaging of induction of a selective Nrf2 target, GFP-tagged Srxn1, and the altered nuclear translocation dynamics of a subunit of NF-kB, GFP-tagged p65, upon TNFR signalling induced by TNFα using HepG2 cells. Strong activation of GFP-Srxn1 expression by DILI compounds typically correlated with suppression of NF-κB nuclear translocation, yet reversely, activation of NF-κB by TNFα did not affect the Nrf2 response. DILI compounds that provided strong Nrf2 activation, including diclofenac, carbamazepine and ketoconazole, sensitized towards TNFα-mediated cytotoxicity. This was related to an adaptive primary protective response of Nrf2, since loss of Nrf2 enhanced this cytotoxic synergy with TNFα, while KEAP1 down regulation was cytoprotective. These data indicate that both Nrf2 and NF-κB signalling may be pivotal in the regulation of DILI. We propose that the NF-κB inhibiting effects that coincide with a strong Nrf2 stress response likely sensitize liver cells to pro-apoptotic signalling cascades induced by intrinsic cytotoxic pro-inflammatory cytokines.

**Keywords:** Drug-induced liver injury; live-cell imaging; Nrf2 activation; oxidative stress; NF-κB signalling

## 2. Introduction

Drug safety issues that lead to drug-induced liver injury (DILI) are the major reason for drug-related hospitalizations and drug withdrawals. Often with no overt changes in hepatocellular toxicity parameters (e.g. rise in alanine or aspartate aminotransferase (ALT/AST) levels or increased total bilirubin) found in pre-clinical settings, drugs are (unknowingly) safely marketed until more than 1 in 10,000 drug users demonstrate signs of liver failure [6]. Novel, predictive systems for DILI based on mechanistic understanding will be essential to pave the way forward for improved drug safety assessment.

The common notion around DILI is that drugs affect the intracellular biochemistry of liver cells, either elicited by the parent drug, its metabolites or the metabolic shift the drug conveys upon uptake [6, 281]. Although often idiosyncratic there is a need to understand the key events that are critical mechanistic determinants of human DILI. Perturbations of immune mediated signalling seems an important event in DILI [282]. In particular, TNFα-mediated signalling seems an important contributor to sensitize liver cells to drug-induced hepatocyte toxicity both in vitro [244] as well as in vivo [283]. TNFα mediates intracellular signalling through activation of NF-κB transcription factor [284]. NF-κB transiently translocates to the nucleus to activate downstream (cytoprotective) target genes including chemokines, inhibitor of apoptosis proteins family members (IAPs) and anti-apoptotic Bcl2 family members [285]. We demonstrated that for diclofenac the synergy with TNFα to kill hepatocytes is directly related to inhibition of NF-κB

nuclear translocation and activation, and that inhibition of NF-κB signalling sensitizes towards cytotoxicity caused by diclofenac [38].

Bioactivation of drugs contributes to the formation of reactive metabolites which is shown to be a risk factor in DILI [286]. These reactive metabolites typically provoke a cellular oxidative stress environment thereby initiating the stabilization and activation of the transcription factor Nrf2 [287]. Subsequent downstream target gene activation by Nrf2 contributes to adaptation and protection of cells against oxidative stress. Likewise Nrf2 deletion in the liver severely increases the sensitivity towards drug-induced liver failure [113, 288]. In some studies it has been shown that Nrf2 activation can act to suppress NF-κB-based immune signalling responses [289] which is interesting as this would suggest Nrf2 could be involved in NF-κB suppression in certain situations including DILI. So far there is no systematic evaluation on the relationship between Nrf2 and NF-κB activation in DILI.

Here we investigated whether drugs with known risk of DILI invoke specific cellular stress and defense pathways (NF-κB and Nrf2) that predict the degree of drug toxicity and whether associations between these pathways exist. We investigated the transcriptional response to 90 DILI-associated drugs as well as several cytokines/growth factors in primary human hepatocytes (PHH) at multiple concentrations and time-points, based on publicly available data [70]. To translate these findings to high throughput approaches we established novel GFP-based reporter cell lines to quantitatively assess Nrf2 and NF-kB activation on a cell-to-cell basis and amenable for high content high throughput live-cell imaging. Our combined data indicate that the degree of oxidative stress in liver cells negatively correlates with NF-κB activity and that the inability to adequately respond to inflammatory responses upon drug exposure predisposes liver cells towards cell death. We propose that our integration of live cell high content imaging models to determine Nrf2 and NF-kB activation as well as cytotoxicity is likely to contribute to improve the discrimination of novel drug entities that are intrinsically at risk for DILI.

## 3. Materials and Methods

### 3.1. Reagents

All drugs were acquired from Sigma-Aldrich and freshly dissolved in DMSO, except for menadione and naproxen (in PBS). Human TNFα was purchased from R&D systems and stored as 10 µg/mL in 0.1% BSA in PBS aliquots.

### 3.2. Cell culture

Human hepatoma HepG2 cells were acquired from ATCC (clone HB8065) and maintained and exposed to drugs in DMEM high glucose supplemented with 10% (v/v) FBS, 25U/mL penicillin and 25µg/mL streptomycin. The cells were used between passage 5 and 20. For live cell imaging, the cells were seeded in Greiner black µ-clear 96 wells plates, at 20,000 cells per well.

### 3.3. Gene expression analysis.

CEL files were downloaded from the Open TG-GATEs database for all DILI-related compounds (see Supplementary Table 1): “Toxicogenomics Project and Toxicogenomics Informatics Project under CC Attribution-Share Alike 2.1 Japan” http://dbarchive.biosciencedbc.jp/en/open-tggates/desc.html. Probe annotation was performed using the hthgu133pluspmhsentrezg.db package version 17.1.0 and Probe mapping was performed with hthgu133pluspmhsentrezgcdf

downloaded from NuGO (http://nmg-r.bioinformatics.nl/NuGO_R.html). Probe-wise background correction (Robust Multi-Array Average expression measure), between-array normalization within each treatment group (quantile normalization) and probe set summaries (median polish algorithm) were calculated with the rma function of the Affy package (Affy package, version 1.38.1). [228] The normalized data were statistically analyzed for differential gene expression using a linear model with coefficients for each experimental group within a treatment group. [258]

A contrast analysis was applied to compare each exposure with the corresponding vehicle control. For hypothesis testing the empirical bayes statistics for differential expression was used followed by an implementation of the multiple testing correction of Benjamini and Hochberg[254] using the LIMMA package [259].

### 3.4. Cluster analysis of oxidative stress and inflammation regulated gene sets.

A gene set for oxidative stress and a gene set for inflammatory signalling was generated using several databases (see Supplementary Fig 1). From Ingenuity Pathway Analysis (version 18841524) the genes present in the following pathways were extracted: NRF2-mediated Oxidative Stress Response, Death Receptor Signalling, NF-κB Signalling, TNFR1 Signalling, TNFR2 Signalling and Toll-like Receptor Signalling. From the Gene Ontology project [290], genes associated with the following terms were obtained using AmiGO 2 version: 2.2.0 [291]. For oxidative stress: "response to oxidative stress" GO:0006979 and for inflammatory signalling: "regulation of inflammatory response" GO:0050727, both queries with filters evidence type closure: “experimental evidence” and taxon closure label: “Homo sapiens”.

From the Molecular Signatures Database (MSigDB) [292] the following genesets from BioCarta “BIOCARTA NRF2 PATHWAY” for oxidative stress and “BIOCARTA NFKB PATHWAY”, “BIOCARTA DEATH PATHWAY”, “BIOCARTA TNFR1 PATHWAY", “BIOCARTA TNFR2 PATHWAY” and “BIOCARTA TOLL PATHWAY” for inflammatory signalling.

From Kyoto Encyclopedia of Genes and Genomes (KEGG Release 71.0, July 1, 2014): [293]. “NF-kappa B signalling pathway”, “TNF signalling pathway” and “Toll-like receptor signalling pathway” for inflammatory signalling. No entry for Nrf2 or oxidative stress was found. From Reactome (Version 48) [294] “innate immune system” and “detoxification of reactive oxygen species” for the inflammatory and oxidative stress signalling, respectively. From “TRANSFAC® (www.biobase-international.com/transcription-factor-binding-sites) from BIOBASE

Corporation” [295] the genes bound by factor NFE2L2 and RELA. From all databases a total of 490 and 175 unique genes were obtained for inflammatory and oxidative stress signalling, respectively. As a next step to determine if the selected genes are actively transcribed in Primary Human Hepatocytes (PHH) of the TG-GATES dataset another selection step was performed using the oxidative stress model compounds diethyl maleate and butylated hydroxyanisole and inflammatory model treatments TNFα, LPS and interleukin 1β; both for the high dose 8 hours and 24 hours data. The oxidative stress gene-set was filtered based on a multiple testing corrected p-value of 0.05, minimum average expression of 5 (log2) and a minimum absolute log2 fold change of 1.5 within the oxidative stress model compound subset resulting in 55 genes. The inflammatory signalling gene-set was filtered based on a multiple testing corrected p-value of 0.05, minimum average expression of 5 (log2) and a minimum absolute log2 fold change of 2 within the inflammatory signalling model treatment subset resulting in 82 genes. The log2 fold change values

for all DILI treatments and controls were gathered followed by manhattan distance measure and ward clustering using the NMF package (version 0.20.5) [227]. Different log2 fold change threshold values were used to obtain similar gene-set sizes.

The DILI-Score annotation was adapted from a manual literature survey performed by Astrazeneca [241]. The DILI concern and SeverityScore was largely based on a text mining study of FDA-labels [264]

### 3.5. Ingenuity Pathway Analysis

Differentially expressed genes for all DILI compounds in the TG-GATEs dataset were selected based on a minimal log2 fold change of 1.3 (fold change of 2.5 X with respect to matched control), a maximum multiple testing corrected p-value of 0.05 and a minimum average log2 expression of 7 within the treatment groups (Supplementary Fig 1) Classification of the selected genes according to their biological and toxicological functions were generated through the use of QIAGEN's Ingenuity Pathway Analysis (IPA®, QIAGEN Redwood City, www.qiagen.com/ingenuity)" which finds associated canonical pathways based on the selected gene sets. P-values are calculated using right-tailed Fisher Exact Test and represented as –log10 (p-values). The p-values were extracted for the "Nrf2-mediated oxidative stress response" pathway representing oxidative stress and as representation for "inflammatory signalling" the average of the p-values of pathways "Toll-like receptor signalling", "death receptor signalling", "TNFR1 signalling", "TNFR2 signalling" and "NF-kB signalling" was calculated. For each treatment the average magnitude of the log2 fold change values of the genes responsible for the significance of the oxidative stress and inflammatory pathways was calculated and displayed as an arrow vector above the –log10 p-value bars of the bargraph. The number of genes responsible for the significance of the individual pathways is color coded from blue (low number of genes) to pink (high number of genes).

### 3.6. Generation of GFP-tagged cell lines

HepG2 cells stably expressing human GFP-p65 as described in [38]. Mouse sulfiredoxin (Srxn1) was tagged with GFP at the C-terminus using BAC recombineering [13] and stably introduced into HepG2 cells by transfection and 500 μg/ml G-418 selection.

### 3.7. RNA interference

siRNAs against human NFE2L2 (Nrf2) and KEAP1 were acquired from Dharmacon (ThermoFisher Scientific) as siGENOME SMARTpool reagents, as well as in the form of four individual siRNAs. HepG2 cells were transiently transfected with the siRNAs (50nM) using INTERFERin (Polyplus) as described previously [38].

### 3.8. Western blotting

Samples were collected by direct cell lysis (including pelleted apoptotic cells) in 1x sample buffer supplemented with 5% v/v β-mercaptoethanol and heat-denatured at 95°C for 10 minutes. The separated proteins were blotted onto PVDF membranes before antibody incubation in 1% BSA in TBS-Tween20. Antibodies: mouse-anti-GFP (Roche); rabbit-anti-IκBα (Cell Signalling); rabbit-anti-Nrf2 (H300, Santa-Cruz); mouse-anti-Cleaved Caspase-8 (Cell Signalling); rabbit-anti-PARP (Cell Signalling); mouse-anti-Tubulin (Sigma); mouse-anti-actin (Santa-Cruz).

### 3.9. Microscopy

Real-time cell death induction was determined by monitoring the accumulation of Annexin-V-Alexa633 labeled cells over a 24 hour time period [261]. For this, transmission and Alexa633 images of the same area with cells were taken automatically every 30 minutes using a BD Pathway™ 855 bioimager with CCD camera and a 10x objective with an image resolution of 608X456 (binning 2).

Accumulation of Srxn1-GFP or nuclear oscillation of GFP-p65 was monitored using a Nikon Eclipse Ti confocal microscope (lasers: 488nm and 408nm), equipped with an automated stage, Nikon 20x Dry PlanApo VC NA 0.75 objective and perfect focus system. Images were acquired at 512X512 pixels. Prior to imaging at >20x magnification, HepG2 cells were loaded for 45 minutes with 100ng/mL $Hoechst_{33342}$ to visualize the nuclei, upon which the Hoechst-containing medium was washed away to avoid Hoechst phototoxicity [224]. Srxn1-GFP cells were imaged every 30 minutes across a 24 hour time span, GFP-p65 cells every 6 minutes for 6 hours.

### 3.10. Image quantification

To quantify the total pixel area occupied by cells or the number of cells per field imaged, transmission images and Hoechst images respectively were analyzed using ImagePro 7.0 (Media Cybernetics). The accumulation of dead cells or the appearance of Srxn1-GFP positive cells was quantified as the total number of pixels above background. The Annexin-V-positive pixel total was normalized for the total cell area. The number of adjacent fluorescent Srxn1-GFP pixels above background (with a minimum size of 45 pixels, which is about 1/4th of average cell size) was multiplied by the average density of those pixels as a measure for the GFP signal-intensity increase and normalized for the amount of nuclei.

To quantify the nuclear translocation of GFP-p65, nuclei (Hoechst) masks are segmented and tracked in ImageJ to define the GFP-p65 nuclear intensity, followed by cytoplasm segmentation. The normalized nuclear / cytoplasmic intensity ratio for each cell is recorded and further analyzed for different oscillation features, also using ImageJ, including the number of translocations, time period of each individual peak, intensity of the peaks, delay between peaks, and nuclear entry and exit rates [296].

### 3.11. Statistics

All experiments are performed at least in triplicate. Error bars indicate Standard Error. Statistical comparisons were done in a one-way ANOVA. P-value indications: $P<0.05$ (*); $P<0.01$ (**); $P<0.001$ (***).

## 4. Results

### 4.1. Enhanced Nrf2 activation is associated with suppression of endogenous NF-κB activity in PHH.

The Japanese Toxicogenomics Project has generated the Open TG-GATEs data repository of gene expression profiles in primary human hepatocytes (PHH) upon exposure to 157 compounds of which many are DILI-related, at 1-3 different concentrations and 1-3 time points (2, 8 and 24 hr), including a few pro-inflammatory cytokines, TNFα, IL1β and LPS [70]. We focused on the NF-κB and Nrf2 signalling related gene sets extracted from several key databases as described in detail the material and methods section. Ingenuity Pathway Analysis (IPA) for oxidative stress and inflammatory signalling was determined for all DILI compounds in the dataset. Typically a significant modulation of these pathways was observed. A major modulation of the "Nrf2-mediated oxidative stress response" overall related to upregulation of genes linked to this pathway. Interestingly, DILI compounds that showed a strong oxidative stress response also showed a modulation of "inflammatory signalling" related to NF-κB activity (26 compounds, $p<0.05$) although this was typically associated with down regulation of genes (Fig.1A). This effect was strongest after 24 hour treatment, although a similar association was already observed at 8 hour treatment (Supplementary Fig. 2A).

The above observation indicated an opposite direction of Nrf2-mediated signalling versus NF-kB-related inflammatory signalling by DILI compounds in PHH. Indeed, Nrf2 can negatively affect NF-κB activity [297, 298]. Therefore we next performed a more detailed hierarchical clustering analysis of the altered gene expression induced by all DILI compounds associated with both signalling pathways. As a first step based on different annotation databases we systematically selected a set of Nrf2 signalling-related genes as well as a set of inflammatory signalling related genes. To determine which genes are responsive to oxidative stress and inflammatory stimuli in PHH we included a stringent filtering procedure based on the exposures of PHH in the TG-GATEs data to diethyl maleate and butylated hydroxyanisole for Nrf2 signalling, and TNFα, IL-1β and LPS for inflammatory signalling. We then extracted the differential expression levels for all DILI compounds for the selected 55 and 82 genes related to Nrf2 signalling and inflammatory signalling, respectively. Using an unsupervised hierarchical clustering for all genes and DILI compounds at 24 hour we could clearly distinguish Nrf2 clusters (A', B', C' and E') and NF-κB gene clusters (D', F' and G') (Fig. 1B). Moreover, cytokines and LPS (cluster A) clearly induced a different response compared to all DILI compounds (clusters B-E). DILI compound cluster C gave the strongest overall response both at the level of Nrf2 target gene activation as well as inflammation signalling target gene down regulation; this cluster was slightly enriched in compounds that demonstrate 'fatal hepatotoxicity'. These effects were not as prominent at 8 hour treatment conditions (Supplementary Fig. 2B).

Within the hierarchical cluster analysis two strong gene clusters were prominent in their response to DILI compounds: a first cluster (cluster B') with Nrf2 target genes that were mostly upregulated by DILI compounds but hardly affected by cytokines, including Maff, Srxn1, Txnrd1, GCLM, SQSTM1, G6PD, FOS, MMP1 and HMOX1, mostly prototypical Nrf2 target genes (see Fig. 2 for examples); and a second cluster (clusters F' and G') with inflammatory genes that were strongly upregulated by the cytokines and LPS, but were strongly downregulated by the same DILI compounds that caused upregulation of Nrf2 targets, and included CXCL1, CCL2, BCL2A1, CXCL11,

CXCL2; (see Fig. 2 for examples). To determine the correlation with the DILI severity, we performed a similar cluster analysis for only severe DILI compounds and non-severe DILI compounds based on the FDA drug labeling classification [264] (Supplementary Figs. 3 and 4). Severe DILI compounds mostly mimicked the overall DILI hierarchical cluster analysis showing the strongest inverse relationship between Nrf2 activity and NF-κB suppression and included diclofenac, sulindac, ketoconazole and acetaminophen.

Altogether these findings indicate a strong correlation between the ability of DILI compounds to induce an adaptive Nrf2 response and the suppression of NF-κB activity.

***Figure 1:*** **Gene expression analysis of 24 hours highest concentration primary human hepatocyte subset of the TG-GATES dataset.** (A) Differentially expressed genes were analyzed with ingenuity pathway analysis as described in detail in the material and methods section. In the top panel the $-\log_{10}$ p-values for the corresponding pathways are displayed for the Nrf2-mediated oxidative stress response. The top panel displays the mean of the p-values for the inflammatory related pathways. Compounds are ordered according to highest significance of the Nrf2-mediated oxidative stress response. The compound labels in red are the compounds chosen in this study. The color of the bars correspond to DILI-severity type or to the oxidative stress/ inflammatory model-compounds (model-compound type). The length of the arrows correspond to the mean fold change of the genes which are responsible for the significance of the corresponding pathways. The direction of the arrow corresponds to either mean up- or down-regulation of these genes. The color of the arrows corresponds to the number of these genes ranging from 10 to 60 genes. (B) Unsupervised hierarchical clustering of all DILI compounds and a selected gene set as described in detail in the material and methods section. Blue corresponds to down- regulated genes and orange to up-regulated genes, the brightness corresponds to the magnitude of the fold changes. The top color-coded bar corresponds to the DILI-Concern or model-compound type. The second top color-coded bar corresponds to the Severity Class or model-compound type. The left color-coded bar corresponds to the gene type- either inflammatory genes, oxidative genes or both. Important clusters on gene-level are represented from A` to H`, and important compound-level clusters with A-E for easy reference from the text. Compounds used in this study are color-coded in red.

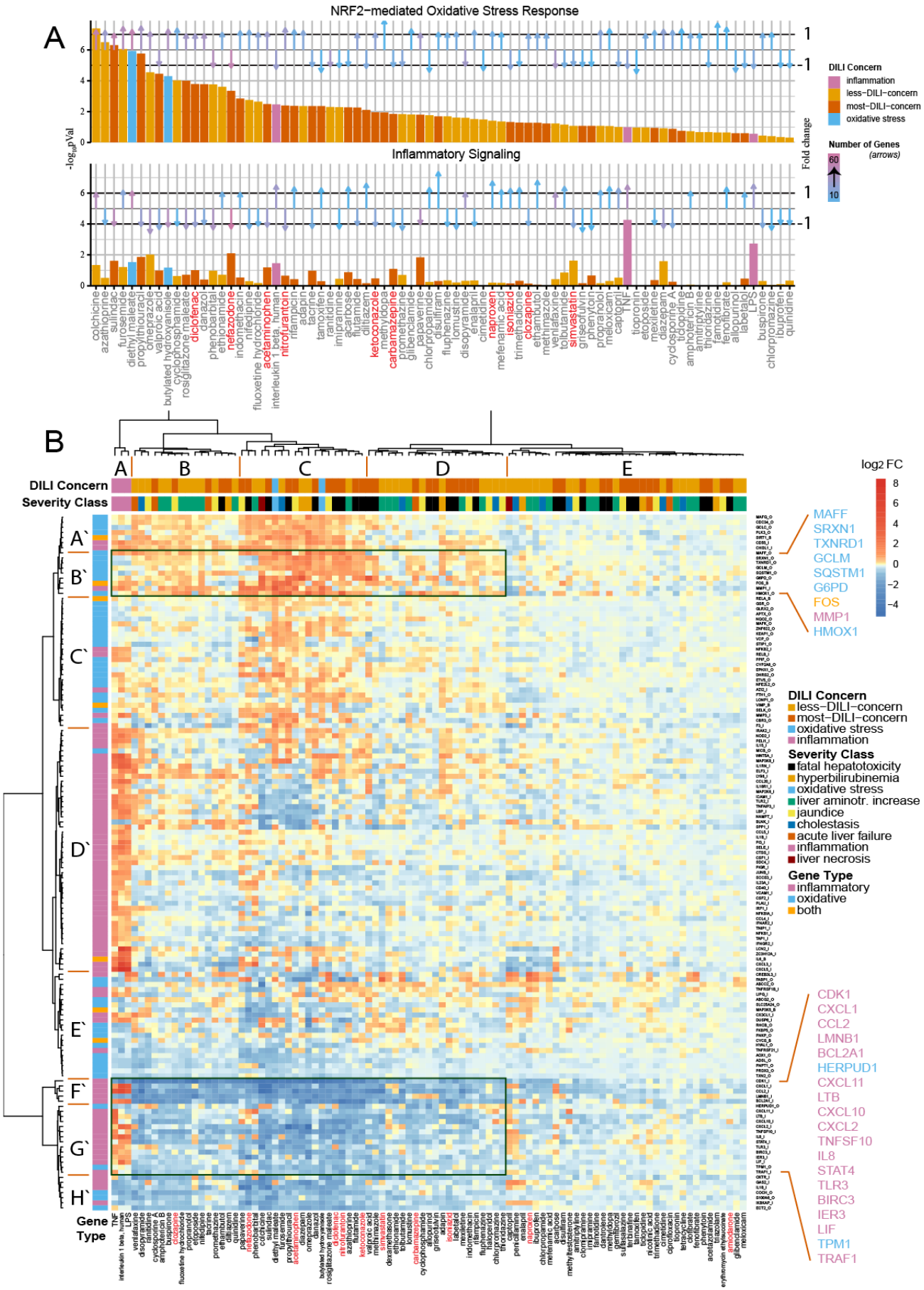
A
NRF2−mediated Oxidative Stress Response
Inflammatory Signaling
-log10pVal
Fold change
DILI Concern
inflammation
less−DILI−concern
most−DILI−concern
oxidative stress
Number of Genes
(arrows)
60
10
colchicine
azathioprine
sulindac
furosemide
diethyl maleate
propylthiouracil
omeprazole
valproic acid
butylated hydroxyanisole
cyclophosphamide
rosiglitazone maleate
diclofenac
clarithromycin
phenobarbital
ethionamide
nefazodone
indomethacin
nifedipine
fluoxetine hydrochloride
acetaminophen
interleukin 1 beta, human
nitrofurantoin
rifampicin
adapin
tamoxifen
ranitidine
imipramine
acarbose
diltiazem
ketoconazole
methyldopa
carbamazepine
gliclazide
glibenclamide
papaverine
chlorpropamide
disulfiram
fluphenazine
lomustine
disopyramide
enalapril
cimetidine
naproxen
mefenamic acid
isoniazid
trimethadione
clozapine
ethambutol
methimazole
venlafaxine
tolbutamide
simvastatin
griseofulvin
primaquine
propranolol
meloxicam
captopril
TNF
tiopronin
etoposide
mexiletine
diazepam
cyclosporine A
ticlopidine
amphotericin B
amitriptyline
thioridazine
famotidine
fenofibrate
allopurinol
labetalol
LPS
buspirone
chlorpromazine
ibuprofen
quinidine
B
A
B
C
D
E
DILI Concern
Severity Class
log2 FC
8
6
4
2
0
−2
−4
A`
B`
C`
D`
E`
F`
G`
H`
MAFF
SRXN1
TXNRD1
GCLM
SQSTM1
G6PD
FOS
MMP1
HMOX1
DILI Concern
less−DILI−concern
most−DILI−concern
oxidative stress
inflammation
Severity Class
fatal hepatotoxicity
hyperbilirubinemia
oxidative stress
liver aminotr. increase
jaundice
cholestasis
acute liver failure
inflammation
liver necrosis
Gene Type
inflammatory
oxidative
both
CDK1
CXCL1
CCL2
LMNB1
BCL2A1
HERPUD1
CXCL11
LTB
CXCL10
CXCL2
TNFSF10
IL8
STAT4
TLR3
BIRC3
IER3
LIF
TPM1
TRAF1
Gene Type

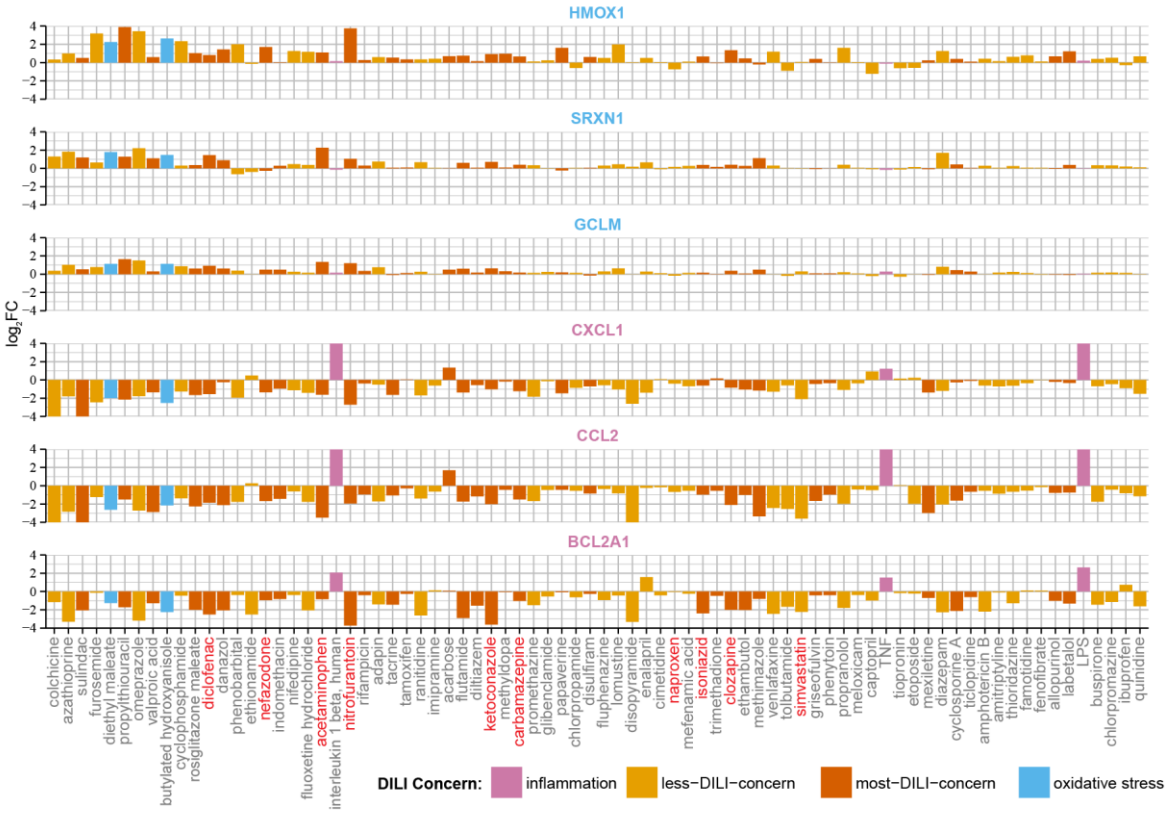


***Figure 2:*** **Fold changes of example genes from the two prominent clusters from the unsupervised hierarchical cluster analysis.** Oxidative stress genes HMOX, SRXN1, GCLM (blue) from cluster B' from Fig. 1B and inflammatory genes CXCL1, CCL2, BCL2A1 (purple) from clusters F'& G'. Color codes are as in Fig. 1.

### 4.2. A BAC-Srxn1-GFP HepG2 cell line reports xenobiotic-mediated Nrf2 activation.

The most prominent differences between NF-κB and Nrf2 responses in the PHH dataset were observed at high concentrations and at 24 hours of drug exposure. Like all signalling events, the transcriptional activity of Nrf2 and NF-κB are dynamic in nature and may show differential activity over time. Therefore we sought to monitor the activity of these two transcription factors in living cells using GFP-tagging technology allowing their dynamic analysis. As PHH dedifferentiate within 24h *in vitro* when grown in 2D cultures [299] and are not amenable for stable expression of GFP reporter constructs, we chose the liver model cell line HepG2 to generate stable fluorescent reporters for both NF-κB and Nrf2 signalling. As a first step, to enable reliable quantitative measurements of the dynamic effect of drug exposure on Nrf2 activity using live cell imaging, we generated a HepG2 reporter cell line based on bacterial artificial chromosome (BAC) recombineering [48] of the Nrf2 target gene sulfiredoxin (Srxn1) [13] which was part of the predictive DILI cluster. We tagged the Srxn1 gene with GFP at its C-terminus and established a stably expressing HepG2 Srxn1-GFP cell line under control of its own entire promoter region. To monitor for its functionality as an Nrf2 reporter, we exposed the HepG2 cells to menadione (20 µM, MEN) and di-ethyl maleate (100 µM, DEM) as proto-typical model activators of Nrf2, as well as diclofenac and ketoconazole, of which the PHH data revealed their capacity to strongly activate an Nrf2 response. DEM, MEN, DCF and KTZ all stabilized Nrf2 levels in our cells (Fig. 3B & C). Live-cell imaging by confocal microscopy followed by automated image quantification showed that the Srxn1-GFP reporter is activated with different kinetics by different compounds with MEN and DEM

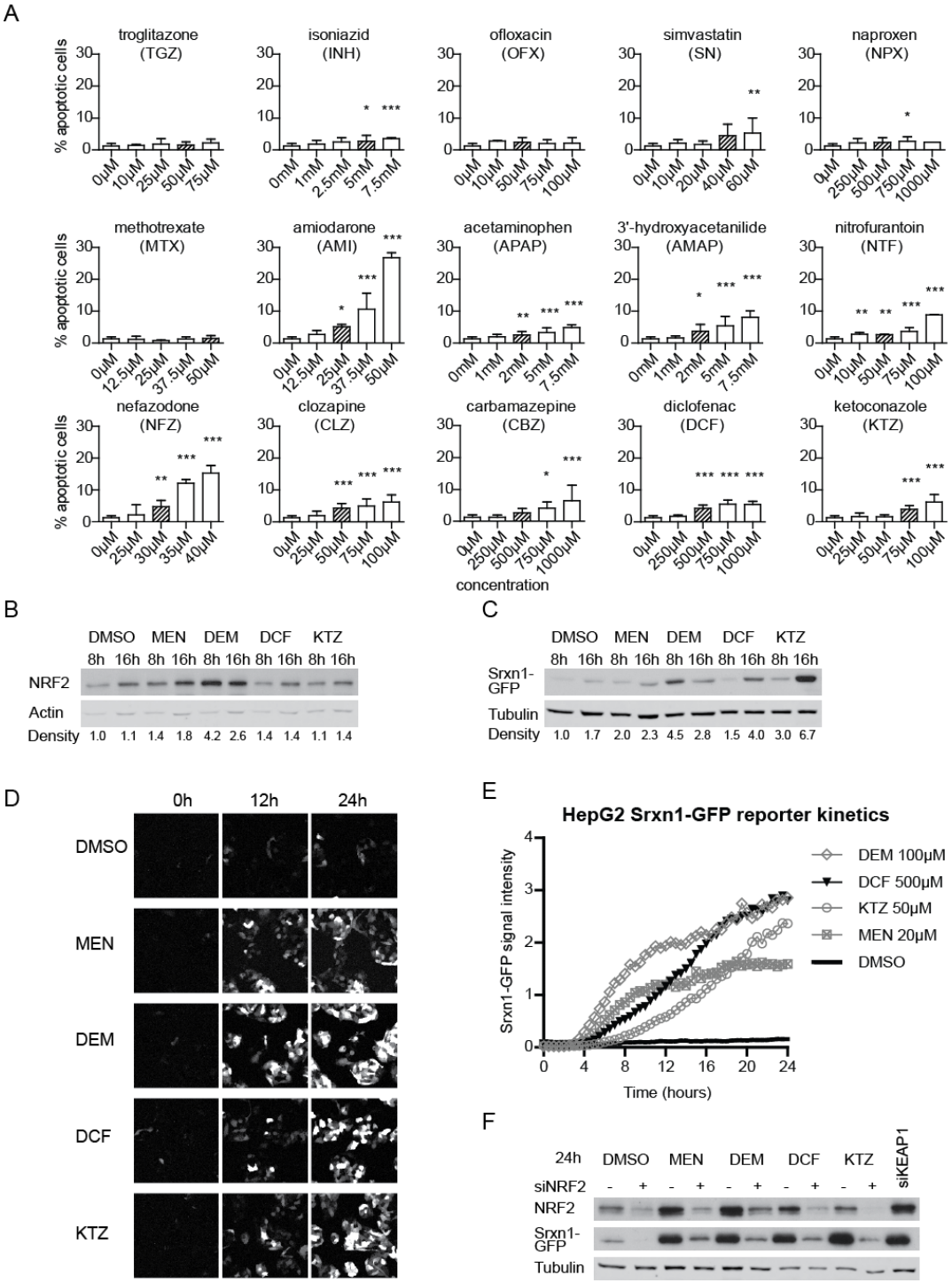


***Figure 3:*** **Srxn1-GFP BAC HepG2 reporter cell line is dependent on Nrf2/KEAP1 signalling.** (A) Cell injury assay using Annexin-V-Alexa-633 staining after 24 hour exposure to our compound set. (B) Western blot of Nrf2 expression in HepG2 cells exposed for 8 or 16 hours to menadione (MEN), diethyl-maleate (DEM), diclofenac (DCF) or ketoconazole (KTZ). Density quantification is relative to Actin levels, normalized to DMSO. (C) Western blot of GFP expression in HepG2 Srxn1-GFP cells as in (B). Density quantification below is relative to tubulin levels. (D) Stills of time-lapse imaging of HepG2 Srxn1-GFP cells exposed to Nrf2 inducers. (E) Quantification of the Srxn1-GFP reporter response kinetics. (F) siRNA-mediated knockdown of Nrf2 (+ siNrf2) or KEAP1 (siKEAP1) or mock treatment (-) in HepG2 Srxn1-GFP cells exposed to DMSO, MEN, DEM, DCF or KTZ for 24h.

being fast inducers, likely related to their direct mode-of-action, and diclofenac and ketoconazole showing a delayed response, possibly related to bioactivation (Fig.3B-E); this effect was directly

related to the expression of the GFP-Srxn1 fusion product. Finally, to confirm that our Srxn1-GFP reporter is under direct control of the KEAP1/Nrf2 pathway, we transiently transfected the HepG2 Srxn1-GFP cells with siRNA oligos targeting Nrf2 or KEAP1. siRNA targeting Nrf2 prevented the stabilization of Nrf2 and consequently inhibited the Srxn1-GFP induction for all compounds. In contrast, as expected KEAP1 knock down itself stimulated Srxn1-GFP expression (Fig. 3F). These data show that the Srxn1-GFP signal intensity depends on the functional KEAP1/Nrf2 pathway.

### 4.3. Drug-induced cell death of human HepG2 cells.

Next we selected a set of DILI compounds for further characterization. Since the opposite regulation of Nrf2 versus NF-κB by DILI compounds was largely seen for severe DILI compounds that often require bioactivation, we selected a small panel of compounds that was contained within the TG-GATEs dataset (acetaminophen (APAP), carbamazepine (CBZ), clozapine (CLZ), diclofenac (DCF), ketoconazole (KTZ), nitrofurantoin (NTF) and nefazadone (NFZ)) as well as some DILI compounds that do not require bioactivation and do not activate the Nrf2 pathway much in PHH (amiodarone (AMI), naproxen (NPX) and simvastatin (SN)); we further complemented our compound set with a few additional drugs that fit in these categories but were not included in the TG-GATEs (ofloxacin (OFX), isoniazid (INH), methotrexate (MTX), 3'-hydroxyacetanilide (AMAP) and troglitazone (TGZ)) (Supplementary Table 2). We first tested whether these compounds induced sufficient cell injury that resulted in cell death at similar concentrations as used for the PHH dataset (Fig. 3A). Based on automated live cell imaging of Annexin-V positive cells we identified concentration-dependent HepG2 cell death for AMI, APAP, AMAP, CBZ, CLZ, DCF, KTZ, NFZ, NTF and SN. Little cell death was observed for INH, MTX, NPX, OFX and TGZ. For further experiments we continued with a mildly cytotoxic concentration (<10 % apoptosis onset) for each compound (indicated in Supplementary Fig. 5) to establish the effect on Nrf2 activation, NF-κB signalling and the cytotoxic interaction between DILI compounds and the pro-inflammatory cytokine TNFα.

### 4.4. DILI compounds activate the Nrf2 stress response independent of TNFR activation.

The PHH dataset predicted that APAP, CBZ, CLZ, DCF, KTZ and NTF potently activate the Nrf2 response; that INH, NFZ and NPX mildly induce Nrf2 and that AMI and SN weakly activate it (Supplementary Fig. 6). Using live-cell imaging we tested whether these same drugs activated the Srxn1-GFP response in HepG2 cells (Fig. 4A-B). We observed that APAP induced the oxidative stress reporter as soon as 4 hours after compound exposure, which is remarkable considering the low CYP2E1 levels in HepG2 cells however this does indicate that the HepG2 is sensitive to oxidative stress-adaptation signalling. Possibly APAP induces oxidative stress through other means than CYP2E1-mediated bioactivation, possibly involving direct modulation of the mitochondrial respiratory chain. NTF, DCF, KTZ, CLZ, CBZ and NFZ strongly induced the Srxn1-GFP reporter as early as 8 hours after compound exposure. AMI, MTX and NPX showed weak Srxn1-GFP induction with delayed kinetics, around 16 hours after compound exposure. INH, OFX, SN and TGZ did not lead to oxidative stress induction within the 24 hour imaging period in our cell system. These

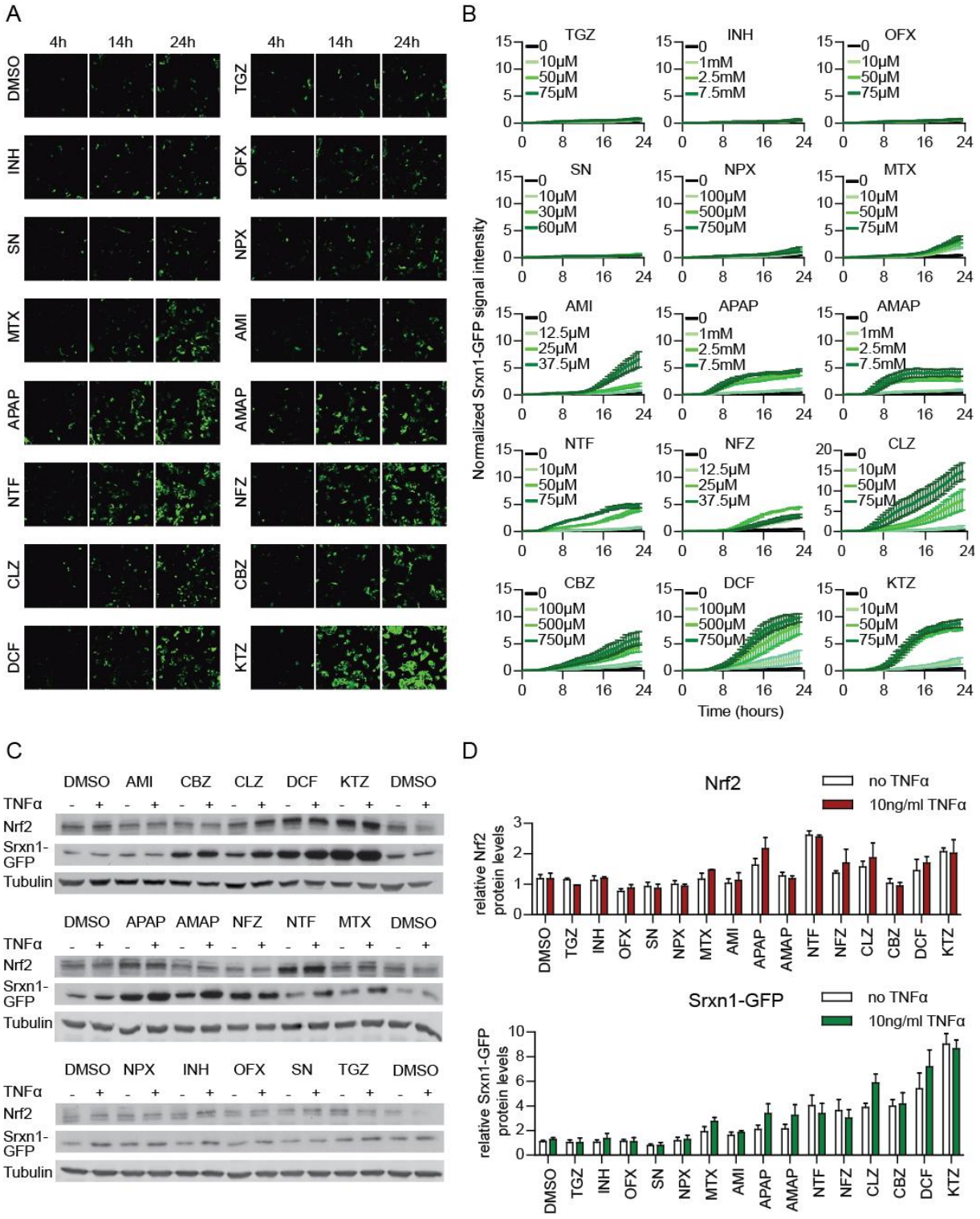


***Figure. 4:*** **Drug exposure induces dynamically divergent Nrf2 responses.** (A) Stills of confocal live-cell imaging in HepG2 Srxn1-GFP cells upon drug exposure (shown are 4, 14 and 24 hours). (B) Quantification of the Srxn1-GFP signal appearing upon exposure to increasing drug doses (averages shown of 4 independent replicates). (C) Western-blots for Nrf2 and GFP expression after 24 hour drug exposure in HepG2 Srxn1-GFP cells, either with or without co-exposure to 10ng/ml TNFα. (D) Quantification of the Nrf2 and Srxn1-GFP protein levels, 24h after drug +/- TNFα exposure (averages of 3 replicates).

findings indicate that the PHH results on the Nrf2 pathway activation correlate well with the HepG2 Srxn1-GFP reporter cell observations.

TNFα promotes NF-κB target gene activation through binding to TNFRSF1A. TNFα binding to its receptor has been suggested to promote Nrf2 activation [300], while the PHH dataset predicted no effect of TNFα on Nrf2 responses. To confirm this we tested whether drug exposure in combination with 10 ng/mL TNFα influenced the drug-induced Nrf2 response (Fig. 4C and D). We observed neither a significant rise nor a decrease in Nrf2 stabilization or Srxn1-GFP expression at 24h when the HepG2 Srxn1-GFP cells were exposed to TNFα alone or in combination with an 8 hour drug pre-exposure. This suggests that TNFα-mediated NF-κB signalling does not influence Nrf2 target gene activation caused by deleterious DILI compounds.

### 4.5. DILI compounds cause a perturbation of NF-κB signalling.

To test whether Nrf2 activation by DILI compounds is associated with modulation of NF-κB signalling, we made use of a previously established HepG2 cell line expressing GFP-tagged p65/RelA, a subunit of the dimeric transcription factor NF-κB [38]. As reported [38], an 8 hour DCF pre-exposure delays the second translocation event (peaking 26 minutes later than vehicle pre-incubated cells) (Fig. 5A). Also NTF (+29 minutes), KTZ (+26 minutes), AMI (+22 minutes), NFZ (+22 minutes) and CBZ (+20 minutes) delayed the oscillation to a similar extent as DCF. Pretreatment with CLZ and MTX only weakly perturbed the appearance of the second translocation response with a delay of 12 and 9 minutes, respectively. Neither AMAP, APAP, INH, OFX, SN nor TGZ significantly influenced the translocation maximum of the second nuclear translocation event.

Our live cell imaging approach allowed detailed cell population-based quantitative analysis of the translocation response to extract various relevant parameters that describe the NF-κB oscillation pattern invoked by TNFα at the single cell as well as the cell population level [296]. This analysis revealed that pre-treatment with AMI, CBZ, DCF, KTZ, NFZ or NTF significantly delayed the time between the first and second NF-κB nuclear translocation maxima that normally occur at 30 minutes and 150 minutes after TNFα exposure, respectively (Fig. 5B). This effect limits the average number of translocation events observed within the 6 hour imaging window (Fig. 5C). Importantly, by evaluating on average ~1,000 cells per condition, we identified that AMI, CBZ, DCF, KTZ, NFZ and NTF induced a sharp decrease in the percentage of cells that undergo three or more NF-κB nuclear translocation events (Fig. 5D). Together, the results indicate that various DILI compounds affect the TNFα-induced NF-κB activation response by modulating its nuclear translocation dynamics. For the compounds with this delayed translocation event the NF-κB target genes are down regulated (Fig. 1A) and all compounds except amiodarone fall within inhibited NF-κB/ activated Nrf2 signalling clusters (clusters B-C, and CBZ cluster D, Fig. 1B) suggesting that the delayed translocation could be indicative for lower NF-κB target gene expression.

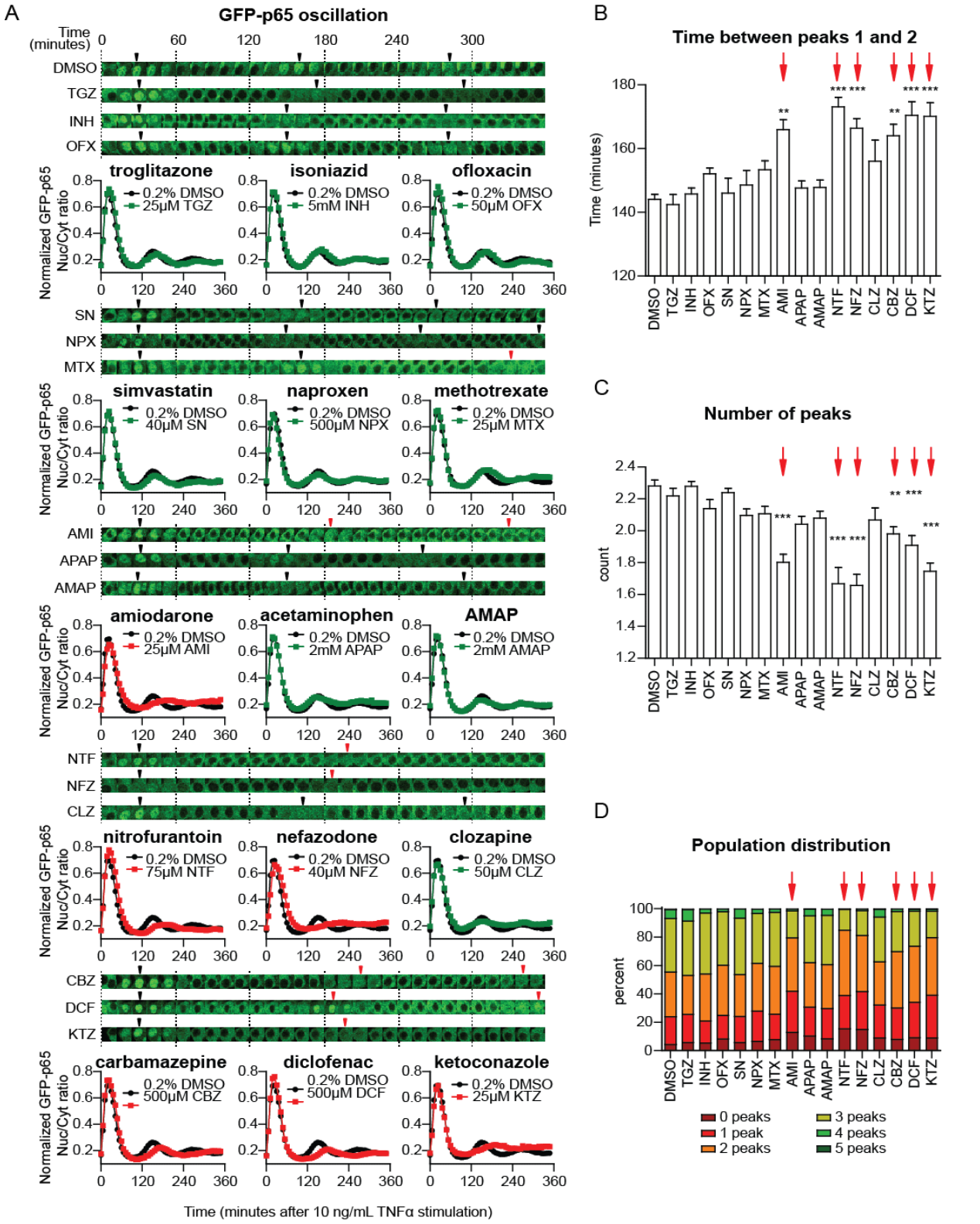


***Figure. 5*: DILI compounds affect the TNFα-mediated nuclear translocation response of NF-κB.** (A) Time-lapse images of one cell that illustrates NF-κB oscillation upon 10ng/ml TNFα stimulation after an 8 hour drug pre-incubation period. Arrowheads point at the local nuclear translocation maxima ("peaks"). Quantified average of the GFP-p65 nuclear/cytoplasmic intensity ratio (average of 3 experiments, totaling 800-1200 cells), normalized between 0 and 1 to focus on the appearance of the nuclear translocation maxima. (B) Analysis of the NF-κB response: time between peaks 1 and 2. (C) Analysis of the NF-κB response: assessment of the number of peaks. (D) Distribution of the TNFα-stimulated, drug pre-exposed cell population, classified for showing 0 to 5 peaks within the 6 hour imaging period.

### 4.6. The inhibitory effect of Nrf2 activity on NF-κB signalling promotes the pro-apoptotic role of TNFα in drug-exposed HepG2 cells.

TNFα-mediated signalling seems important in DILI [244, 282]. While TNFα-receptor mediated NF-κB signalling may provide survival signalling through the upregulation of anti-apoptosis genes such as the anti-apoptotic Bcl-2 family member A1 (BCL2A1), activation of the TNFR may in parallel initiate activation of caspase-8 and thereby switch on apoptosis[301]. Since DILI compounds did affect the NF-kB signalling, and therefore possibly suppressed survival signalling, we next investigated whether DILI compounds would also predispose to the onset of TNFα-mediated apoptosis. To address this issue we monitored the rate of HepG2 cell apoptosis by live-cell imaging with Annexin-V-Alexa633 after 8 hour drug pre-exposure and tested whether TNFα co-exposure enhanced the apoptotic response at 24 hours. TNFα enhanced the apoptosis induction upon CBZ and DCF exposure by 18.6% and 9.7% respectively. A smaller increase of 3 to 4% in cell death upon TNFα co-stimulation was found for KTZ, AMI, NFZ and CLZ (Fig. 6A and 6B). Since TNFα-mediated death signalling acts through caspase-8 activation, we anticipated that the synergy for the onset of apoptosis would also be associated with enhanced caspase-8 cleavage. Caspase-8 was markedly increased by TNFα combined with CBZ and DCF, yet for other DILI compounds tested such a caspase-8 activation was not observed, as was expected based on the limited onset of apoptosis (Fig. 6C and 6D). The enhanced caspase-8 cleavage was associated with cleavage of PARP, a well-established caspase substrate which serves as a pivotal marker of onset of apoptosis. This indicates that primarily under CBZ and DCF pretreatment conditions co-treatment with TNFα turns on apoptosis.

***Table 1*: Summary of DILI compound modulation of Nrf2 and NF-kB signalling and onset of DILI compound/TNFα cytotoxic synergy.** Full names, abbreviations and function of the drugs chosen for this study. The DILI classification was derived from Chen et al. 2011. The overall results from the current study are summarized as fold induction of the Srxn1-GFP intensity compared to control (Nrf2 response), timing of the GFP-p65 assay, focusing on the delay in the second nuclear translocation event upon TNFα exposure (NF-κB response) and percentage of dead cells as observed by the Annexin-V live assay (including TNFα-enhanced cell death).

| Drug name | Abbreviation | Function | DILI label / score | DILI classification | DILI type | DILI concern | Nrf2 response assay (fold induction) | NF-κB oscillation delay upon TNFα | Apoptosis assay ( + last 16h TNFα) | Apoptosis effect of TNFα (% increase) | Nrf2 Transcripts up & NfKb Transcripts down |
|---|---|---|---|---|---|---|---|---|---|---|---|
| troglitazone | TGZ | antidiabetic | N.A. | N.A. | Acute - cholestatic injury | Most | 1.3x | 2 min | 1.1% (2.6%) | 1.5 | N.A |
| isoniazid | INH | antimycobacterial drug | B.W. 8 | Fatal hepatotoxicity | Acute - hepatocellular injury | Most | 1.0x | 2 min | 2.8% (3.3%) | 0.5 | 2-9 |
| ofloxacin | OFX | antibiotic | N.A. | N.A. | Acute - hepatocellular injury | Less | 1.1x | 8 min | 2.3% (3.2%) | 0.9 | N.A |
| simvastatin | SN | antihyperlipidemic | W/P 3 | Liver aminotransferases increase | Acute - hepatocellular injury | Less | 1.1x | 2 min | 2.5% (3.6%) | 1.1 | 2-19 |
| naproxen | NPX | NSAID | W/P 3 | Liver aminotransferases increase | Acute - cholestatic injury | Less | 1.8x | 4 min | 2.1% (2.3%) | 0.2 | 2-4 |
| methotrexate | MTX | antineoplastic agent | B.W. 3 | Liver aminotransferases increase | Chronic - microvesicular steatosis | Less | 3.3x | 9 min | 1.9% (1.9%) | 0 | N.A |
| amiodarone | AMI | antiarrhythmic agent | B.W. 8 | Fatal hepatotoxicity | Chronic - steatohepatitis | Most | 1.9x | 22 min | 5.8% (9.0%) | 3.2 | 0-0 |
| acetaminophen | APAP | analgesic and antipyretic | W/P 5 | Jaundice | Acute - hepatocellular injury | Most | 4.0x | 4 min | 2.5% (2.5%) | 0 | 12-29 |
| 3'-hydroxyacetanilide | AMAP | regionisomer of paracetamol | N.A. | N.A. | N.A. | Less | 4.0x | 4 min | 3.1% (3.4%) | 0.3 | N.A |
| nitrofurantoin | NTF | antibacterial | W/P 8 | Fatal hepatotoxicity | Chronic - autoimmune hepatitis | Most | 4.6x | 29 min | 2.9% (3.6%) | 0.7 | 15-23 |
| nefazodone | NFZ | antidepressant | B.W. 8 | Fatal hepatotoxicity | Acute - hepatocellular injury | Most | 4.8x | 22 min | 3.5% (6.8%) | 3.3 | 13-20 |
| clozapine | CLZ | antipsychotic drug | W/P 25 | Cholestasis; steatohepatitis | Acute - cholestatic injury | Most | 4.6x | 12 min | 4.0% (7.7%) | 3.7 | 1-12 |
| carbamazepine | CBZ | antiepileptic drug | W/P 7 | Acute Liver Failure | Acute - cholestatic injury | Most | 4.1x | 20 min | 3.9% (22.5%) | 18.6 | 4-9 |
| diclofenac | DCF | NSAID | W/P 8 | Fatal hepatotoxicity | Acute - hepatocellular injury | Most | 6.7x | 26 min | 4.5% (14.2%) | 9.7 | 12-23 |
| ketoconazole | KTZ | antifungal antibiotic | B.W. 8 | Fatal hepatotoxicity | Acute - hepatocellular injury | Most | 8.3x | 26 min | 5.0% (8.1%) | 3.1 | 9-17 |

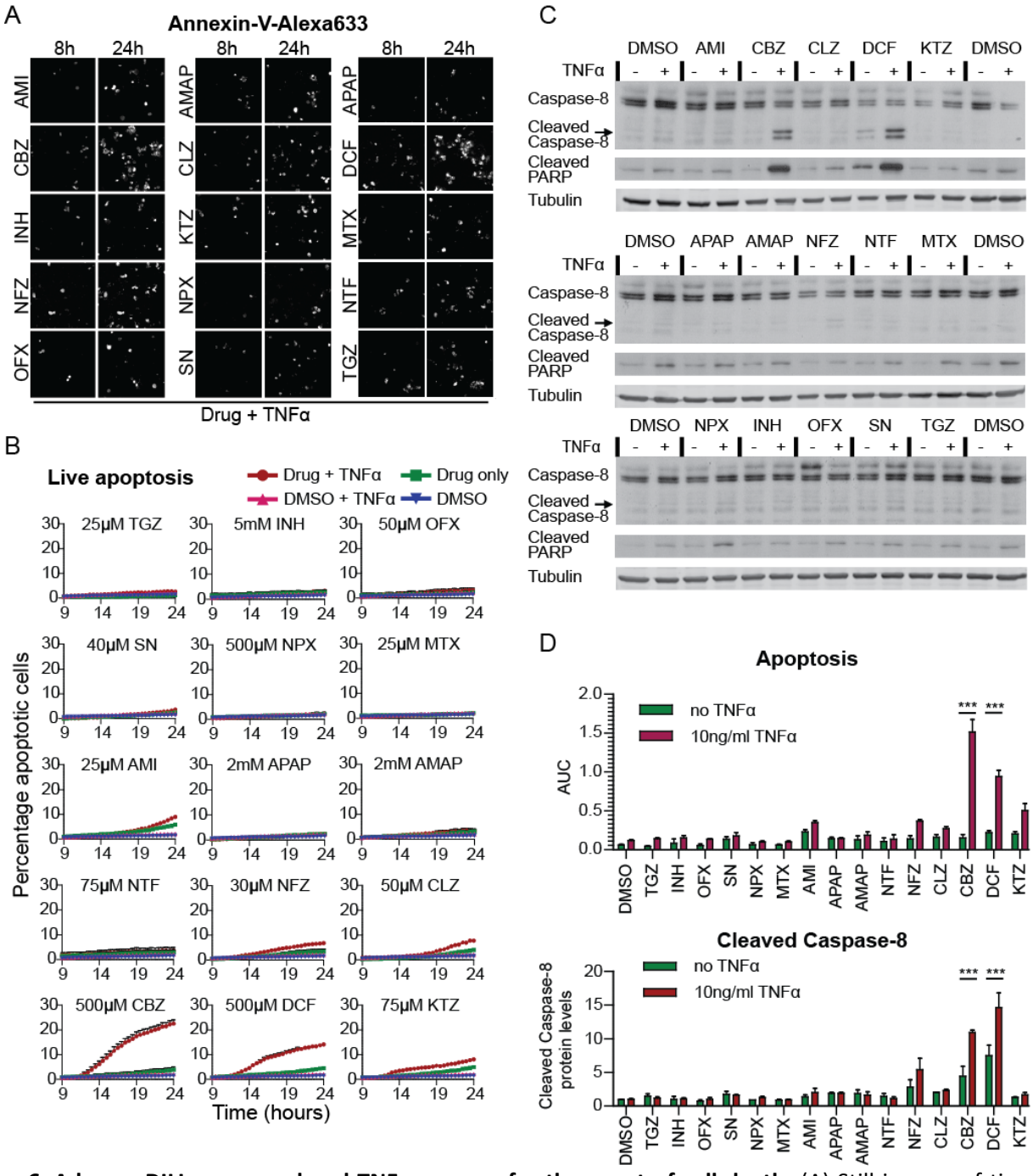


***Figure 6*: Adverse DILI compound and TNFα synergy for the onset of cell death.** (A) Still images of time-lapse movies of HepG2 cells exposed to the drugs in co-presence of Annexin-V-Alexa-633, taken at 8 hours (before 10ng/ml TNFα addition) and at 24 hours (16 hours TNFα). (B) Quantification of the percentage dead cells appearing upon drug only exposure, or in combination with TNFα. Average of 3 to 6 experiments. (C) Western-blot for cleaved caspase-8 and the caspase substrate PARP, induced by 24 hour drug alone or drug-TNFα co-treatment. (D) Comparison of the quantified percentage of dead cells 24 hours after drug (+TNFα) exposure: the appearance of dead cells in live-cell imaging as area under the curve (AUC) (as in B) and quantification of cleaved caspase-8 protein levels (relative density as in C, average of 3 experiments)

## 5. Discussion

Here we focused on the interplay of two pivotal cellular stress response signalling pathways in drug-induced liver injury: TNFα-mediated NF-κB signalling and chemical stress-induced Nrf2 activation. Extensive transcriptomics data from primary human hepatocyte revealed that the Nrf2 transcriptional program is activated by a majority of different DILI compounds in particular those that are associated with severe DILI. This strong Nrf2 activation correlates with a major downregulation of genes that are under the direct control of NF-κB. We successfully transferred this inverse relationship between Nrf2 activation and NF-κB signalling into a panel of GFP-reporter based high content imaging assays, which now allows the high throughput assessment of their dynamic activation [236]. Using live-cell imaging we established the time-profiles of the activation of these transcription factors and established that various DILI compounds activate Nrf2 activity as well as negatively modulate the NF-κB nuclear oscillation response induced by TNFα. Although no cause and effect relationship between these two signalling pathways has been proven in our study, our data do support an overall working model whereby DILI compounds that strongly affect the Nrf2 response as well as modulate the NF-κB oscillatory response (either directly or indirectly) act in synergy with TNFα to cause a cytotoxic response. An integrated automated high throughput microscopy-based platform that simultaneously measures drug-induced Nrf2 activation, TNFα-induced NF-κB activation and cytotoxicity, will likely contribute to the exclusion or de-prioritization of novel drug entities for further development.

Our data indicate a differential regulation of Nrf2 and NF-κB signalling pathways in primary human hepatocytes (PHH). From the Japanese Toxicogenomics Project a total of 90 DILI compounds have been evaluated. While several DILI compounds caused a strong modulation of most Nrf2 and NF-κB target genes, e.g. nitrofurantoin, diclofenac and ketoconazole, the effect of amiodarone was only modest. Despite the fact that HepG2 cells are notorious for their low level expression of CYP enzymes [207], an enhanced formation of reactive intermediates during drug metabolism may be causative for the activation of the Nrf2 response. However, we cannot exclude the role of other stress response pathways that are intricately linked to the modulation of the Nrf2 response and by themselves are activated by chemical-induced cell injury, including the perturbation of the mitochondria, the endoplasmic reticulum (ER) and the autophagosomes which may result in a secondary source of reactive oxygen species that may initiate an adaptive Nrf2 response [302]. Although the role of these other programs will require further mechanistic investigations, our previous investigations demonstrate that suppression of the Nrf2 adaptive stress response strongly sensitizes cells towards a synergistic toxicity with TNFα, indicating that enhanced oxidative stress predisposes for TNFα sensitization [238].

The PHH transcriptomics data indicated that many DILI compounds themselves suppress the activity of NF-κB target genes. In addition, our imaging data indicate that various DILI compounds suppress the NF-κB oscillatory response. Together this suggests that also under control situations the overall nuclear localization of NF-κB may be limited, thereby precluding the activation of NF-κB target genes. Alternatively a limited activation of NF-κB by DILI compounds possibly influences the expression of modulators that act as feedback suppressors of NF-κB activity, such as IkBα/NFKBIA or A20/TNFAIP3 [303]. Indeed, NF-κB signals through an auto-regulatory negative feedback mechanism that essentially desensitizes a cell for a limited time period against re-activation of the response by an active NF-κB inducing kinase complex (IKK) [304]. Although drug exposure alone

may elicit NF-κB oscillations, this does not limit the primary nuclear translocation event upon TNFα exposure, only the subsequent nuclear translocation events. The later oscillations are less intense and less synchronized due to induction of a second negative feedback regulator, A20. Interestingly, several, but not all, DILI compounds affect the expression of IkBα and A20 in PHH, which often occur in parallel, supporting a similar mechanism of activation (see Supplementary Fig. 7). We therefore turned to our GFP-p65 reporter and tested whether the test drugs can induce NF-κB oscillations on their own. In line with this we found that DCF, CBZ, NFZ, CLZ and KTZ induced a limited NF-κB transition in 2-6% of a given cell population within the first two hours after exposure which was not apparently different from control conditions (Supplementary Fig. 8). This suggests that drug pre-exposure does not directly change the initial balance of NF-κB and its cytoplasmic inhibitor, IκBα, but rather may influence the transcriptional and translational responses required for normal execution of the timing of the NF-κB response after the first nuclear translocation event.

The rationale for the choice of drugs was to investigate whether our live-cell imaging systems were able to discriminate between drugs that are often linked to DILI (TGZ, AMI, INH, KTZ, NFZ, MTX, NTF, CBZ and DCF) and relatively safe drugs (NPX, SN, OFX and CLZ). We have focused on NF-κB signalling, Nrf2 activation and cell death induction and a summary of the different responses is provided in Table 1. As APAP and AMAP induce hepatocellular death through necrosis at high levels of drug concentrations (an $EC_{50}$ in PHH of ~25mM), and not apoptosis, these are considered as relatively safe drugs [305]. Based on our results, NPX, SN and OFX are safe (no massive cell death induction, no gross effect on Nrf2 or NF-κB signalling), but clozapine should be re-evaluated: its profile of strong Srxn1-GFP induction, NF-κB delay and slightly higher cell death induced by TNFα co-exposure shows more resemblance to drugs that are more often associated to DILI, such as DCF, CBZ, KTZ, NFZ and NTF.

Our assays have not been able to pick up any mechanistic signs for toxicity for INH and TGZ, two typical idiosyncratic DILI-related drugs (Table 1). The hepatotoxic effect of these two drugs, however, could partly depend on their inhibitory effect on bile acid transport [306, 307], which might only emerge from advanced (3D) hepatocyte culture models [308]. Moreover, lack of strong bioactivation capacity in HepG2 cells could also be a reason why we could not observe any effect for these compounds.

In conclusion, we demonstrate an association between Nrf2 signalling and NF-κB responses in two distinct liver models: PHH and HepG2. Using the live cell imaging of our GFP-based reporter models for Nrf2 and NF-kB signalling we established the inverse relationship between these signalling pathways in relation to DILI compound and TNFα mediated synergistic toxicity. This was only feasible by assessing the quantitative dynamics of the NF-κB responses, underscoring the integration of live cell imaging of stress response pathways in mechanistic studies in relation to DILI assessment.

## Supplementary Materials

***Supplementary table 1:*** **TG-GATES compounds and DILI annotations.**

| compound | conc.(μM) | Severity Class | DILI-Concern | DILI-Score |
|---|---|---|---|---|
| acetaminophen | 5000 | 5 | Most-DILI-Concern | DILI-Reports |
| isoniazid | 10000 | 8 | Most-DILI-Concern | Severe-DILI |
| phenobarbital | 10000 | 3 | Less-DILI-Concern | NA |
| valproic acid | 5000 | 8 | Most-DILI-Concern | Severe-DILI |
| clofibrate | 300 | 3 | Less-DILI-Concern | NA |
| rifampicin | 70 | 8 | Most-DILI-Concern | DILI-Reports |
| omeprazole | 600 | 4 | Less-DILI-Concern | NA |
| indomethacin | 200 | 5 | Most-DILI-Concern | High-Concern |
| chlorpromazine | 20 | 2 | Less-DILI-Concern | DILI-Reports |
| carbamazepine | 300 | 7 | Most-DILI-Concern | High-Concern |
| diclofenac | 400 | 8 | Most-DILI-Concern | High-Concern |
| nitrofurantoin | 125 | 8 | Most-DILI-Concern | High-Concern |
| diazepam | 250 | 4 | Less-DILI-Concern | NA |
| cyclophosphamide | 2000 | 5 | Less-DILI-Concern | NA |
| phenytoin | 60 | 8 | Most-DILI-Concern | NA |
| allopurinol | 140 | 8 | Most-DILI-Concern | NA |
| propylthiouracil | 4000 | 8 | Most-DILI-Concern | NA |
| gemfibrozil | 100 | 3 | Less-DILI-Concern | NA |
| amiodarone | 7 | 8 | Most-DILI-Concern | Severe-DILI |
| sulfasalazine | 150 | 5 | Most-DILI-Concern | NA |
| cimetidine | 300 | 2 | Less-DILI-Concern | NA |
| haloperidol | 20 | 5 | Less-DILI-Concern | NA |
| fluphenazine | 20 | 3 | Less-DILI-Concern | NA |
| thioridazine | 15 | 5 | Less-DILI-Concern | NA |
| adapin | 75 | 4 | Less-DILI-Concern | NA |
| labetalol | 140 | 8 | Most-DILI-Concern | Severe-DILI |
| methyltestosterone | 20 | 2 | Less-DILI-Concern | NA |
| glibenclamide | 20 | 3 | Less-DILI-Concern | DILI-Reports |
| griseofulvin | 20 | 8 | Most-DILI-Concern | NA |
| flutamide | 50 | 8 | Most-DILI-Concern | Severe-DILI |
| azathioprine | 73 | 3 | Less-DILI-Concern | High-Concern |
| ketoconazole | 15 | 8 | Most-DILI-Concern | Severe-DILI |
| tetracycline | 25 | 2 | Less-DILI-Concern | High-Concern |
| lomustine | 120 | 3 | Less-DILI-Concern | NA |
| ciprofloxacin | 25 | 7 | Most-DILI-Concern | NA |
| tamoxifen | 25 | 8 | Most-DILI-Concern | High-Concern |
| methyldopa | 50 | 8 | Most-DILI-Concern | High-Concern |
| methimazole | 10000 | 8 | Most-DILI-Concern | DILI-Reports |
| tacrine | 80 | 7 | Most-DILI-Concern | High-Concern |
| imipramine | 15 | 3 | Less-DILI-Concern | High-Concern |
| amitriptyline | 15 | 5 | Less-DILI-Concern | NA |
| ibuprofen | 150 | 3 | Less-DILI-Concern | DILI-Reports |
| naproxen | 600 | 3 | Less-DILI-Concern | High-Concern |
| quinidine | 50 | 3 | Less-DILI-Concern | NA |
| furosemide | 2500 | 2 | Less-DILI-Concern | DILI-Reports |
| fenofibrate | 30 | 3 | Less-DILI-Concern | NA |
| chlorpropamide | 750 | 2 | Less-DILI-Concern | DILI-Reports |
| nicotinic acid | 10000 | 7 | Most-DILI-Concern | NA |
| erythromycin ethylsuccinate | 5 | 5 | Most-DILI-Concern | NA |
| ethambutol | 4000 | 8 | Most-DILI-Concern | NA |
| mefenamic acid | 150 | 3 | Less-DILI-Concern | NA |
| famotidine | 700 | 3 | Less-DILI-Concern | DILI-Reports |
| ranitidine | 4000 | 5 | Less-DILI-Concern | High-Concern |
| nifedipine | 150 | 3 | Less-DILI-Concern | DILI-Reports |
| diltiazem | 150 | 4 | Most-DILI-Concern | NA |
| captopril | 8000 | 6 | Less-DILI-Concern | NA |
| enalapril | 2000 | 4 | Less-DILI-Concern | High-Concern |
| papaverine | 60 | 5 | Most-DILI-Concern | NA |
| penicillamine | 10000 | 2 | Less-DILI-Concern | NA |
| sulindac | 3000 | 8 | Most-DILI-Concern | High-Concern |
| disopyramide | 3500 | 2 | Less-DILI-Concern | NA |
| mexiletine | 300 | 3 | Most-DILI-Concern | NA |

| | | | | |
|---|---|---|---|---|
| acetazolamide | 600 | 8 | Most-DILI-Concern | NA |
| disulfiram | 60 | 8 | Most-DILI-Concern | High-Concern |
| colchicine | 4000 | 6 | Less-DILI-Concern | NA |
| tolbutamide | 2000 | 2 | Less-DILI-Concern | DILI-Reports |
| acarbose | 10000 | 8 | Most-DILI-Concern | NA |
| simvastatin | 30 | 3 | Less-DILI-Concern | High-Concern |
| meloxicam | 50 | 3 | Less-DILI-Concern | NA |
| ethionamide | 600 | 3 | Less-DILI-Concern | NA |
| ticlopidine | 20 | 4 | Most-DILI-Concern | High-Concern |
| tiopronin | 2000 | 3 | Less-DILI-Concern | NA |
| promethazine | 35 | 5 | Less-DILI-Concern | NA |
| dantrolene | 10 | 8 | Most-DILI-Concern | Severe-DILI |
| clomipramine | 10 | 8 | Most-DILI-Concern | DILI-Reports |
| terbinafine | 15 | 8 | Most-DILI-Concern | High-Concern |
| danazol | 35 | 8 | Most-DILI-Concern | NA |
| etoposide | 330 | 3 | Less-DILI-Concern | NA |
| venlafaxine | 1200 | 7 | Less-DILI-Concern | DILI-Reports |
| clozapine | 50 | 5 | Most-DILI-Concern | High-Concern |
| buspirone | 30 | 3 | Less-DILI-Concern | Transaminitis |
| nefazodone | 30 | 8 | Most-DILI-Concern | Severe-DILI |
| triazolam | 10 | 4 | Less-DILI-Concern | NA |
| trimethadione | 10000 | 5 | Most-DILI-concern | NA |
| cyclosporine A | 6 | 7 | Most-DILI-Concern | NA |
| diethyl maleate | 1500 | oxidative stress | oxidative stress | NA |
| LPS | 300 | inflammation | inflammation | NA |
| TNF | 50 | inflammation | inflammation | NA |
| interleukin 1 beta, human | 50 | inflammation | inflammation | NA |
| butylated hydroxyanisole | 200 | oxidative stress | oxidative stress | NA |
| amphotericin B | 2 | 3 | Less-DILI-Concern | NA |
| fluoxetine hydrochloride | 20 | 3 | Less-DILI-Concern | DILI-Reports |
| dexamethasone | 300 | 3 | Less-DILI-Concern | Transaminitis |
| rosiglitazone maleate | 300 | 5 | Most-DILI-Concern | High-Concern |
| propranolol | 100 | 3 | Less-DILI-Concern | DILI-Reports |

1: steatosis, 2: cholestasis, 3: liver aminotransferases increase, 4: hyperbilirubinemia, 5: Jaundice, 6: liver necrosis, 7: acute liver failure, 8: fatal hepatoxicity

***Supplementary table 2:*** **Drugs used in this study and their reported adverse effects on the liver.**

| Drug name | Abbreviation | Type | Function | Metabolizing enzymes | Adverse drug reactions in the liver | References |
|---|---|---|---|---|---|---|
| amiodarone | AMI | Positive control | antiarrhythmic agent | CYP3A4; 1A2 | ALT/AST elevations; cirrhosis; jaundice; hepatomegaly; hepatitis; phospholipidosis; steatohepatitis; cholestasis | (Lu *et al.*, 2012; Pollak and Shafer, 2004) |
| 3'-hydroxyacetanilide | AMAP | Negative control | regionisomer of paracetamol | CYP2E1 | Does not cause liver failure in mice | (Halmes *et al.*, 1998; Stamper *et al.*, 2010) |
| paracetamol / acetaminophen | APAP | Positive control | analgesic and antipyretic | CYP2E1; 1A2; 2D6; 3A4 | Acute liver failure; necrosis | (Jaeschke *et al.*, 2012; Manyike *et al.*, 2000; Pirmohamed *et al.*, 1996) |
| carbamazepine | CBZ | Positive control | antiepileptic drug | CYP3A4; 2C9; induces CYP3A4 | Drug hypersensitivity; acute hepatitis; ALT/AST elevations; chronic hepatitis | (Bjornsson, 2008; Daly, 2012; Phillips and Mallal, 2011; Syn *et al.*, 2005) |
| clozapine | CLZ | Positive control | antipsychotic drug | CYP3A4; 1A2; 2D6 | ALT/AST elevations; hepatitis; jaundice; necrosis | (Damsten *et al.*, 2008; Dragovic *et al.*, 2010; Hummer *et al.*, 1997; McKnight *et al.*, 2011; Valevski *et al.*, 1998) |
| diclofenac | DCF | Positive control | NSAID | CYP3A4; 2C9 ; 2C8; UGT2B7 | Acute hepatitis; necrosis; autoimmune chronic liver injury | (Boelsterli, 2003; Deng *et al.*, 2009; Fredriksson *et al.*, 2011) |
| isoniazid | INH | Positive control | anti-tuberculosis drug | CYP2E1; inhibits CYP2C9 and 3A4 | ALT/AST elevation; acute hepatitis; chronic hepatitis; necrosis | (Daly and Day, 2012; Srivastava *et al.*, 2010; Zand *et al.*, 1993) |
| ketoconazole | KTZ | Positive control | antifungal antibiotic | CYP3A4; inhibits CYP3A4 and UGT2B7 | acute hepatitis; cholestasis; necrosis | (Bernuau *et al.*, 1997; Kim *et al.*, 2003; Lin *et al.*, 2008) |
| methotrexate | MTX | Negative control | chemotherapeutic agent | aldehyde oxidase; CYP2E1 | ALT/AST elevations; fibrosis; cirrhosis; chronic hepatitis | (Aithal, 2011; West, 1997) |
| nefazodone | NFZ | Positive control | antidepressant | CYP3A4; inhibits CYP3A4 | liver failure; jaundice; hepatitis; hepatocellular necrosis | (Stewart, 2002; Xu *et al.*, 2008) |
| naproxen | NPX | Negative control | NSAID | CYP2C9 | ALT/AST elevations; cholestasis; acute hepatitis | (Ali *et al.*, 2011) |
| nitrofurantoin | NTF | Positive control | antibiotic against urinary tract infections | CYP1A | autoimmune hepatitis; chronic active hepatitis; necrosis | (Boelsterli *et al.*, 2006; Czaja, 2011) |
| ofloxacin | OFX | Negative control | antibiotic | CYP1A2; 2C19 | hepatocellular necrosis; jaundice; hepatitis | (Blum, 1991) |
| simvastatin | SN | Positive control | statin | CYP3A4 | ALT/AST elevations; jaundice; hepatitis | (Bjornsson *et al.*, 2012; Law and Rudnicka, 2006) |
| troglitazone | TGZ | Positive control | antidiabetic | CYP1A1; 2C8; 2C19; 3A4 | fulminant hepatitis; acute liver failure | (Jaeschke, 2007; Kaplowitz, 2005) |

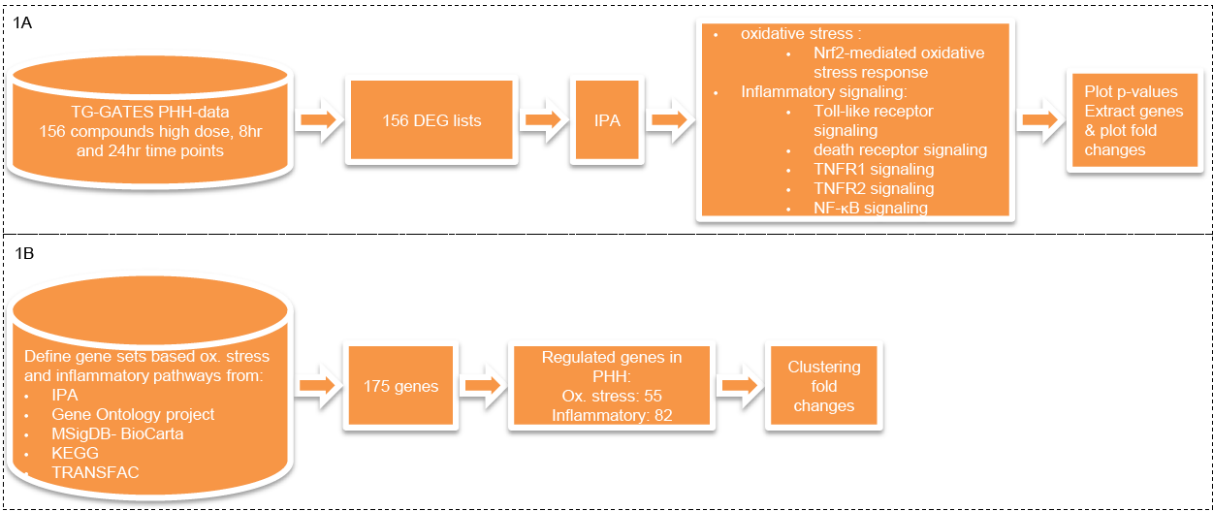


***Supplementary figure 1*: Flow diagram of TG-GATEs informatics analysis.**

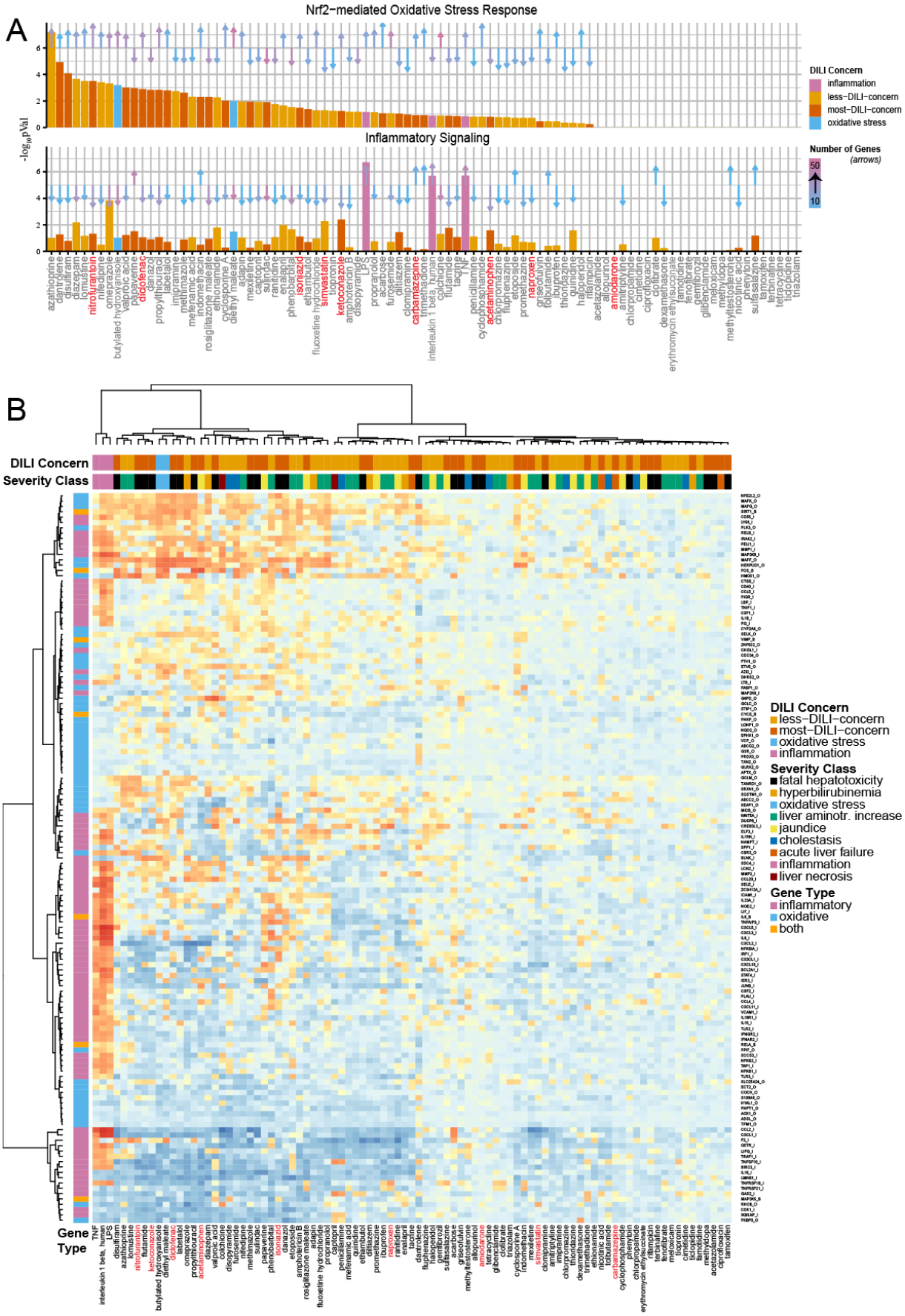


***Supplementary figure 2*: Gene expression analysis of 8 hours highest concentration primary human hepatocyte subset of the TG-GATES dataset.** (A) Differentially expressed genes were analyzed with

Ingenuity Pathway Analysis as described in detail in the material and methods section. In the top panel the $-\log^{10}$ p-values for the corresponding pathways are displayed for the Nrf2-mediated oxidative stress response. The top panel displays the mean of the p-values for the inflammatory related pathways. Compounds are ordered according to highest significance of the Nrf2-mediated oxidative stress response. The compound labels in red are the compounds chosen in this study. The color of the bars correspond to DILI-severity type or to the oxidative stress/ inflammatory model-compounds (model-compound type). The length of the arrows correspond to the mean fold change of the genes which are responsible for the significance of the corresponding pathways. The direction of the arrow corresponds to either mean up- or down-regulation of these genes. The color of the arrows corresponds to the number of these genes ranging from 10 to 50 genes. (B) Unsupervised hierarchical clustering of all DILI compounds and a selected gene set as described in detail in the material and methods section. Blue corresponds to down- regulated genes and orange to up-regulated genes, the brightness corresponds to the magnitude of the fold changes. The top color-coded bar corresponds to the DILI-Concern or model-compound type. The second top color-coded bar corresponds to the Severity Class or model-compound type. The left color-coded bar corresponds to the gene type- either inflammatory genes, oxidative genes or both. Compounds used in this study are color-coded in red.

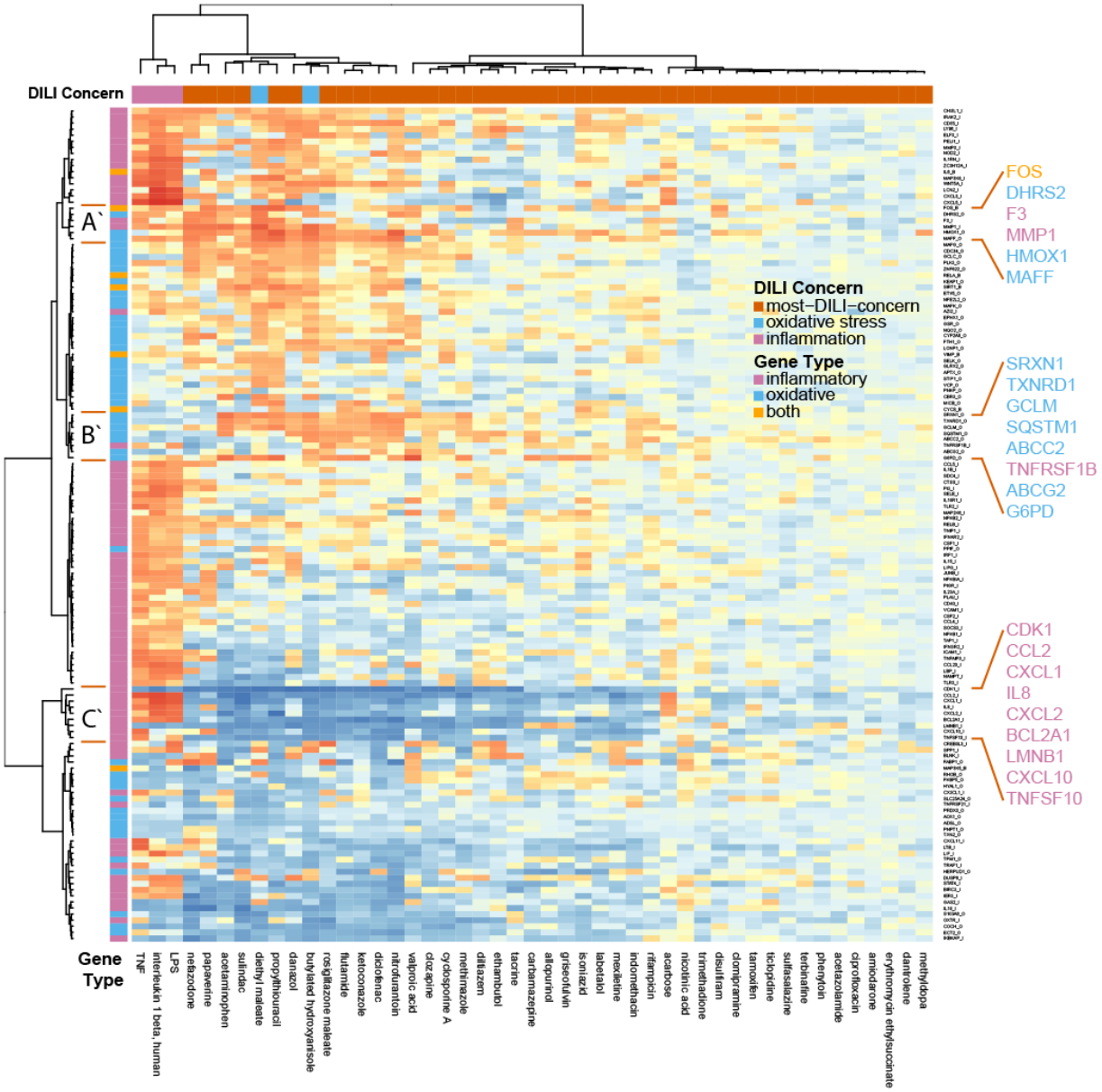

***Supplementary figure 3:*** **Gene expression analysis of Most DILI-concern 24 hours highest concentration primary human hepatocyte subset of the TG-GATES dataset.** Unsupervised hierarchical clustering of most DILI-concern compounds and a selected gene set as described in detail in the material and methods section. Blue corresponds to down- regulated genes and orange to up-regulated genes, the brightness corresponds to the magnitude of the fold changes. The top color-coded bar corresponds to the DILI-Concern or model-compound type. The left color-coded bar corresponds to the gene type- either inflammatory genes, oxidative genes or both.

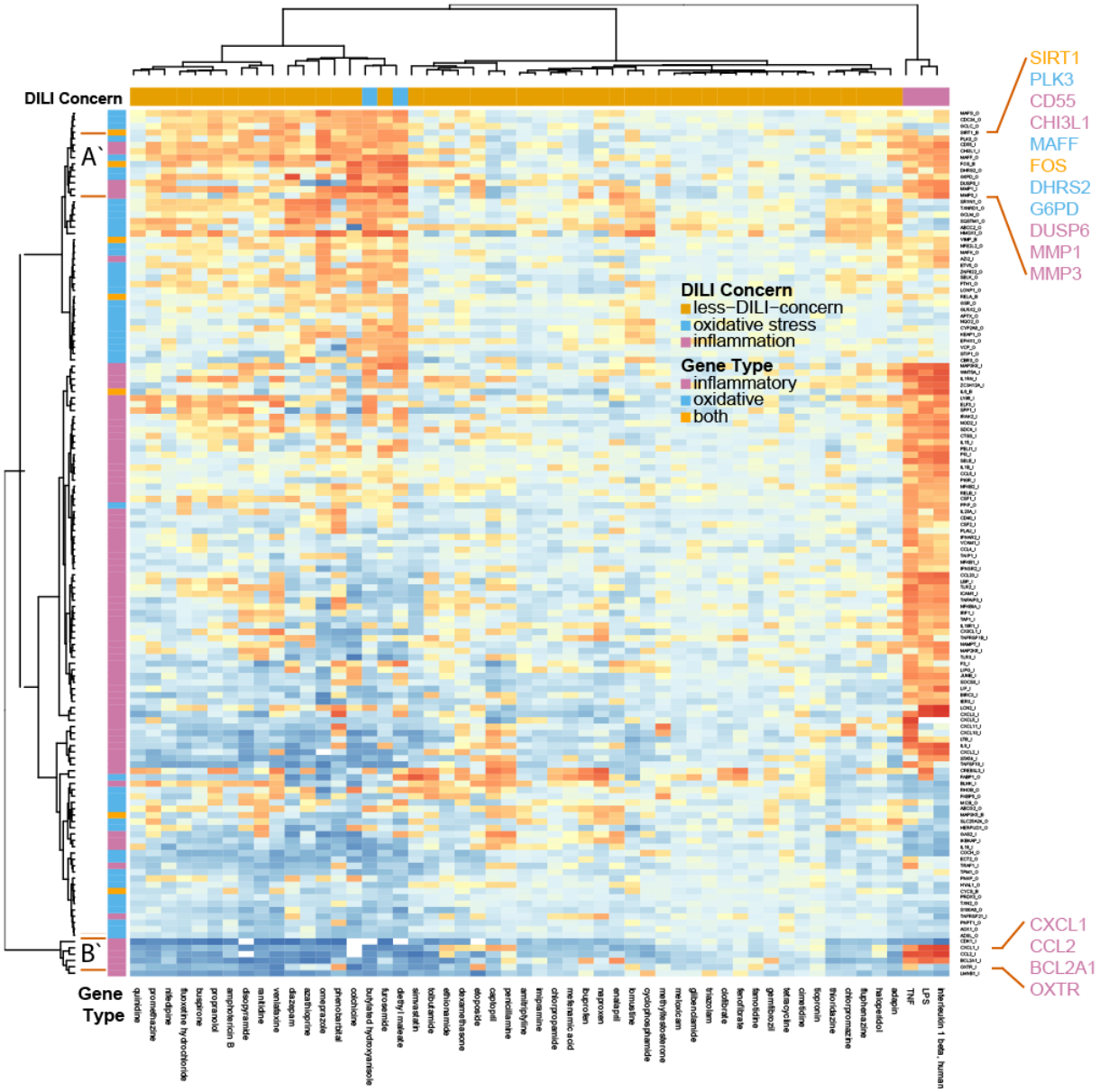


***Supplementary figure 4:*** **Gene expression analysis of Less DILI-concern 24 hours highest concentration primary human hepatocyte subset of the TG-GATES dataset.** Unsupervised hierarchical clustering of less DILI-concern compounds and a selected gene set as described in detail in the material and methods section. Blue corresponds to down- regulated genes and orange to up-regulated genes, the brightness corresponds to the magnitude of the fold changes. The top color-coded bar corresponds to the DILI-Concern or model-compound type. The left color-coded bar corresponds to the gene type- either inflammatory genes, oxidative genes or both.

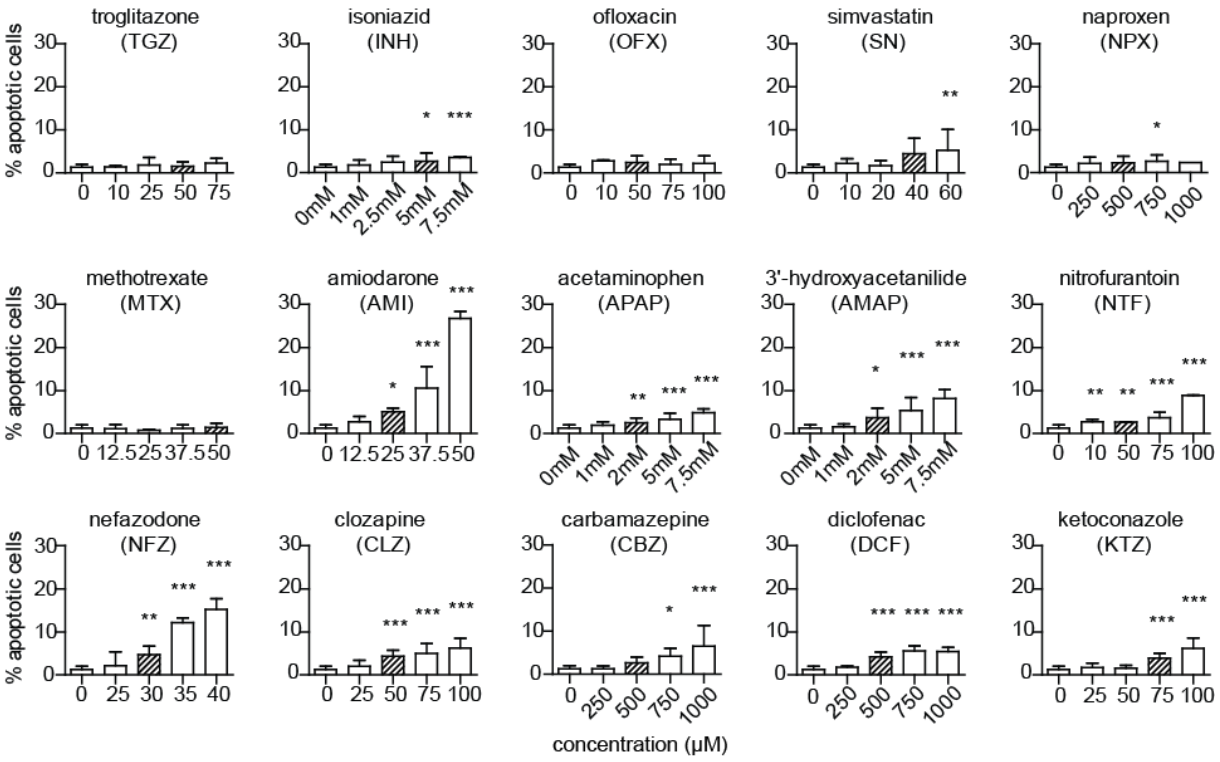


***Supplementary figure 5:*** **Drug-induced cell death of HepG2 cells.** Percentage of dead HepG2 cells at 24 hours after exposure to fifteen different drugs. Concentrations are indicated in μM, except for AMAP, APAP and isoniazid (INH): in mM. "0": 0.2% (v/v) DMSO. Shaded bars: concentration used in subsequent assays.

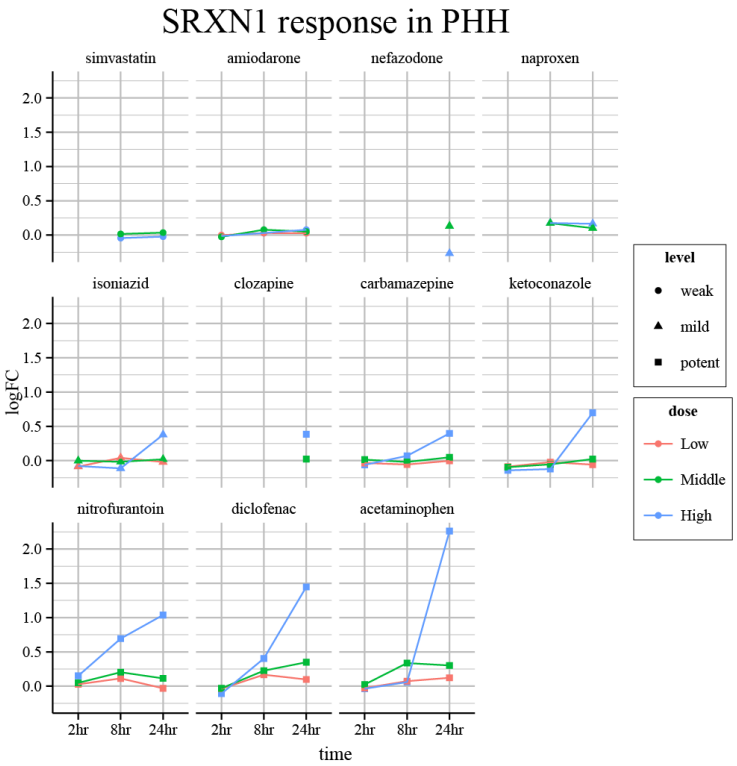


**Supplementary figure 6: Time course fold change of SRXN1 for PHH highest concentration (TG-GATES).** Time course SRXN1 transcript level in PHH cells from the TG-GATES dataset. Fold change is expressed as $log_2$(FC) as compared to matched vehicle controls. The different concentrations are color coded as low (blue), green (Middle) and red (High).

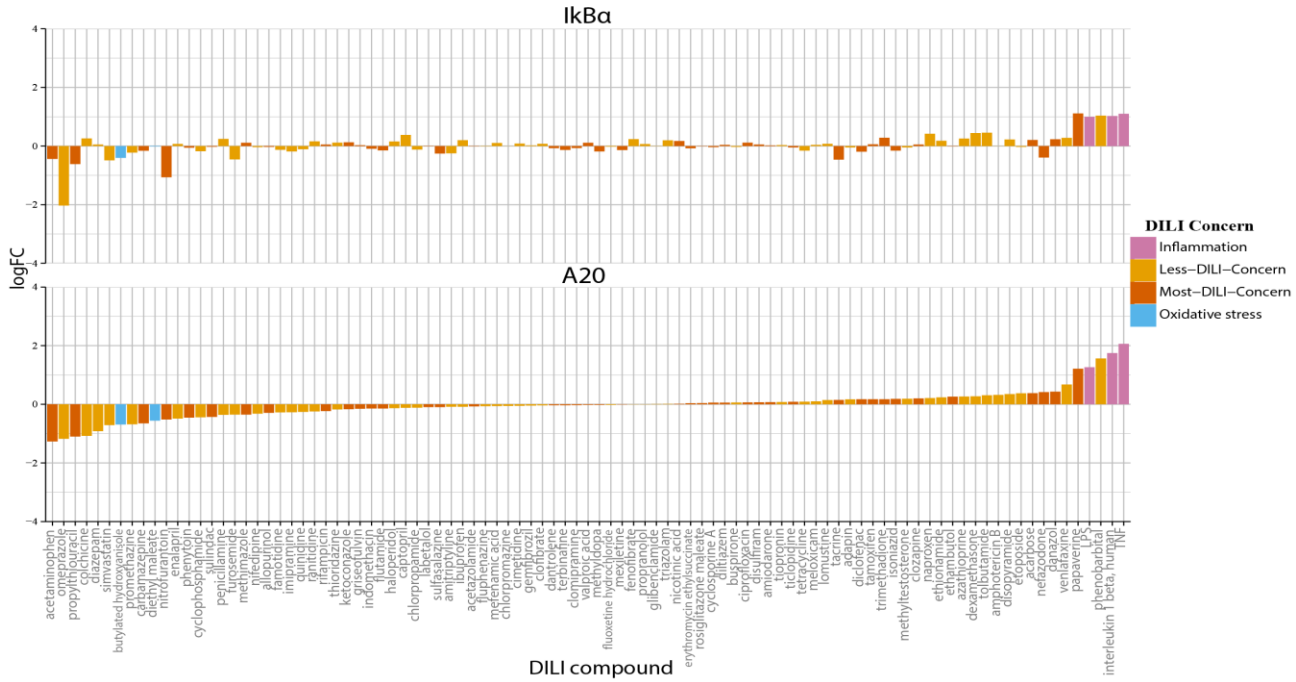


***Supplementary figure 7:*** **Fold change values for IκBα and A20 for PHH highest concentration (TG-GATES).** Fold change is expressed as $\log_2$(FC) as compared to matched controls. Compounds are color coded according to DILI concern: inflammatory model compound (purple), oxidative stress model compound (blue), less-DILI-concern (light orange), most-DILI-concern (dark orange). Compounds are sorted according to $\log^2$(FC) of A20 from low to high.

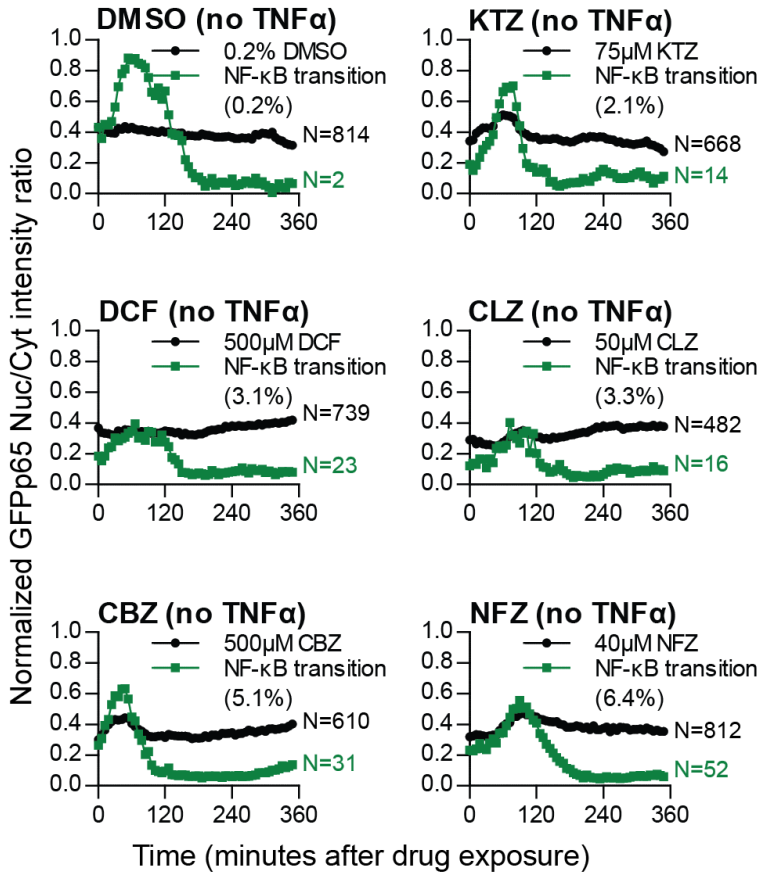


***Supplementary figure 8:*** **Drug-induced GFP-p65 oscillation in HepG2 cells.** Quantified average of the GFP-p65 nuclear/cytoplasmic intensity ratio, normalized between 0 and 1 to focus on the appearance of the nuclear translocation maxima after exposure to 0.2% (v/v) DMSO (solvent control), 50μM CLZ, 500μM DCF, 500μM CBZ, 75μM KTZ and 40μM NFZ. Black line: average population response; Green line: average response of cells that show NF-κB nuclear translocation within the first 2 hours of compound addition.